PALEOCEANOGRAPHY, VOL. 11, NO. 3, PAGES 277-297, JUNE 1996

Messinian deep-water turbidites and glacioeustatic sea-level changes in the North Atlantic: Linkage to the Mediterranean Salinity Crisis

Jijun Zhang and David B. Scott

Centre for Marine Geology, Dalhousie University, Halifax, Nova Scotia, Canada

Abstract. Our benthic foraminiferal data clearly indicate eight layers of deep-water turbidites during the Messinian (MTL 1-8) and one in the early Pliocene (PTL 1) in Ocean Drilling Program Leg 105, Site 646B. These deep-water turbidite deposits are characterized by highly concentrated agglutinated marsh benthic foraminifera (e.g., *Trochammina* cf. *squamata*, *Ammotium* sp. A, *Miliammina fusca*), rounded quartz, polished thick-walled benthic foraminifera, wood fragments, plant seeds, plant fruit, and highly concentrated mica and are interbedded with sediments containing deep-water benthic faunas. We suggest these turbidites deposited during sea-level low stands (~80-100 m below sea level), and their ages are tentatively correlated to 6.59, 6.22, 6.01, 5.89, 5.75, 5.7, 5.65, 5.60, and 5.55 Ma, respectively, based on the Messinian oxygen isotope enrichments at Site 552A of Deep Sea Drilling Project Leg 81. The turbidites layers during the late Messinian, coeval with frequent climate changes suggested by six oxygen enrichment excursions of Site 552A, may have been in part linked to the late Messinian evaporite deposits in the Mediterranean Basin. The most profound climate changes at 5.75 and 5.55 Ma may have been related to the Lower and Upper Evaporites in the Mediterranean Basin.

Introduction

During the Messinian Stage (7.12 to 5.32 Ma) [*Berggren et al.*, 1995], a number of events known as the "Terminal Miocene events" [*Van Couvering et al.*, 1976; *Kennett*, 1983] occurred. These include the Messinian Salinity Crisis, global cooling, and a carbon-13 shift. During the salinity crisis, the Mediterranean Sea became isolated from the world ocean [*Benson and Rakic-El Bied*, 1991], so that a large volume of evaporites was deposited. The origin of these deposits is widely disputed with *Hsü et al.* [1973a, 1973b, 1977, 1978; *Ryan et al.*, 1973] and *Hsü* [1973, 1987, 1988] arguing that the Mediterranean desiccated several times. Their model requires at least 11 episodes during which Atlantic water invaded the desiccated basin. The deposition of these salts could have removed more than 6% of all dissolved salts in the world oceans and turned them less alkaline, causing undersaturation with respect to calcium carbonate and more extensive carbonate dissolution in deep oceans [*Ryan*, 1973].

It was suggested that cooling might have caused increased polar ice sheets and 40-50 m lowering of sea level [*Vail et al.*, 1977; *Hodell and Kennett*, 1986; *Cita and Ryan*, 1978] and 70 m lowering during the late Messinian suggested by *Adams et al.* [1977]. Glacial events may have occurred at 5.2 Ma and 4.8 Ma [*Keigwin*, 1987] (based on the timescale of *Berggren et al.* [1985] and evidence for the earlier glacial has also been recognized in northeastern Morocco and the Southern Ocean [*Hodell et al.*; 1989, *Müller et al.*, 1994; *Hodell et al.*, 1994b]. Also, at this time, evidence from a raised coral atoll of Niue in the South Pacific suggests eight episodes of the sea-level fluctuations occurred with evidence of eight unconformities [*Aharon et al.*, 1993]. A Messinian invasion of cool water planktonic foraminifera in Panama (L. Collins, personal communication, 1995) may have been coeval with glacial expansion in the Arctic [*Ocean Drilling Program Leg 151 Shipboard Scientific Party*, 1994].

The Messinian carbon-13 decrease in deep-sea sediments occurred at ~ 6.3 Ma, slightly after the Messinian/Tortonian boundary at 6.5 Ma (*Berggren et al.* [1985] timescale) [*Loutit and Kennett*, 1979; *Loutit and Keigwin*, 1982; *Keigwin*, 1979, 1987; *Keigwin and Shackleton*, 1980; *Haq et al*; 1980; *Hodell et al*; 1986; *Hodell and Kennett*, 1986; *Hodell et al.*, 1989].

The major cause of the shift observed in both planktonic and benthic foraminiferal records in all ocean basins is equivocal. It was widely suggested that the shift may be linked to sea-level lowering that could have increased the influx of organic matter from the continents into the open oceans as a result of Antarctic glaciation [e.g., *Loutit and Keigwin*, 1982; *Berger and Vincent*, 1986; *Benson et al.*, 1991]. *Bender and Keigwin* [1979] suggested that the ^{13}C shift may indicate a different abyssal circulation pattern before the shift resulting from the shoaling of the Isthmus of Panama or a global decrease in upwelling rate. Other factors, such as increase of bottom circulation rates or an increase in biogenic silica removal in the Southern Ocean high productivity zone have also been considered with respect to the shifted oceanic ^{13}C value [*Loutit and Keigwin*, 1982]. Most recently, *Hodell et al.* [1994a] suggest that the ^{13}C shift may be explained as a result of a net transfer of carbon from terrestrial (land plants and soils) to the oceanic reservoir, because of the shift from C_3-dominated to C_4-dominated ecosystems during the late Miocene. C_4-plants between 6 and 7 Ma may have been related to increased aridity, which

Paper number 96PA00572.
0883-8305/96/96PA-00572$12.00

may have contributed to the onset of negative water budget in the Mediterranean near the Tortonian/Messinian boundary [*Hodell et al.*, 1994a, 1989; *Benson et al.*, 1991].

This paper presents a record of abyssal turbidites delineated by benthic foraminifera, stable strontium, and carbon and oxygen isotopic records from Ocean Drilling Program (ODP) Site 646B and correlated to Deep Sea Drilling Project (DSDP) Leg 81, Site 552A in the North Atlantic Ocean (Figure 1). We reconstruct a sea-level history and evaluate the relationship between the Messinian sea-level fluctuations and the Mediterranean salinity crisis.

Material and Methods

The interval below the lower Pleistocene of the ODP Leg 105, Site 646B was drilled with extended core barrel (XCB) 37% core recovery in average for the Messinian section) on the northern flank of the Eirik Ridge in the southeastern part of the Labrador Sea and southwest of Greenland (58°12.559'N, 48°22.147'W; present water depth 3461.3 m) (Figure 1) [*Srivastava et al.*, 1989a, b]. The location of this hole was chosen to determine the history of paleocirculaton in the North Atlantic and Arctic Oceans, because it is in the region with strong influence from Norwegian-Greenland Sea Overflow Water [*Srivastava et al.*, 1989a]. The whole Messinian section at this site consists of silty clay (69%), clayey silt (11.5%), clay (11%), and nannofossil silty clay and clayey silt (6%) in average. The terrigenous components have been carried along the continental margin of Greenland in a bottom nepheloid layer with periodic contributions from river discharge, low-concentration turbidity currents, or plumes of turbid water originating on the shelf [*Srivastava et al.*, 1989a].

Deep Sea Drilling Project (DSDP) Site 552A (Leg 81) was hydraulically piston cored with almost 100% recovery at the base of Hatton Bank, west margin of the Rockall Plateau (56°02.56'N, 23°13.88'W; present water depth 2301 m; Figure 1). The Hatton Drift is was probably deposited by bottom currents flowing northeastward against the slope of Hatton Bank. The bottom waters at this site lie above the southward flowing North Atlantic Deep Water (NADW) that fills the deeper part of the Iceland Basin and mantles the Reykjanes Ridge south of Iceland [*Roberts et al.*, 1984]. Site 552A contains a continuous upper Miocene-Pliocene sedimentary record, but slumping may have occurred in the Pliocene from cores 17 to 24 [*Stow and Holbrook*, 1984].

Foraminifera

All samples were washed through a 63 μm mesh using tap water and dried in an oven at a temperature of 40°C. Benthic

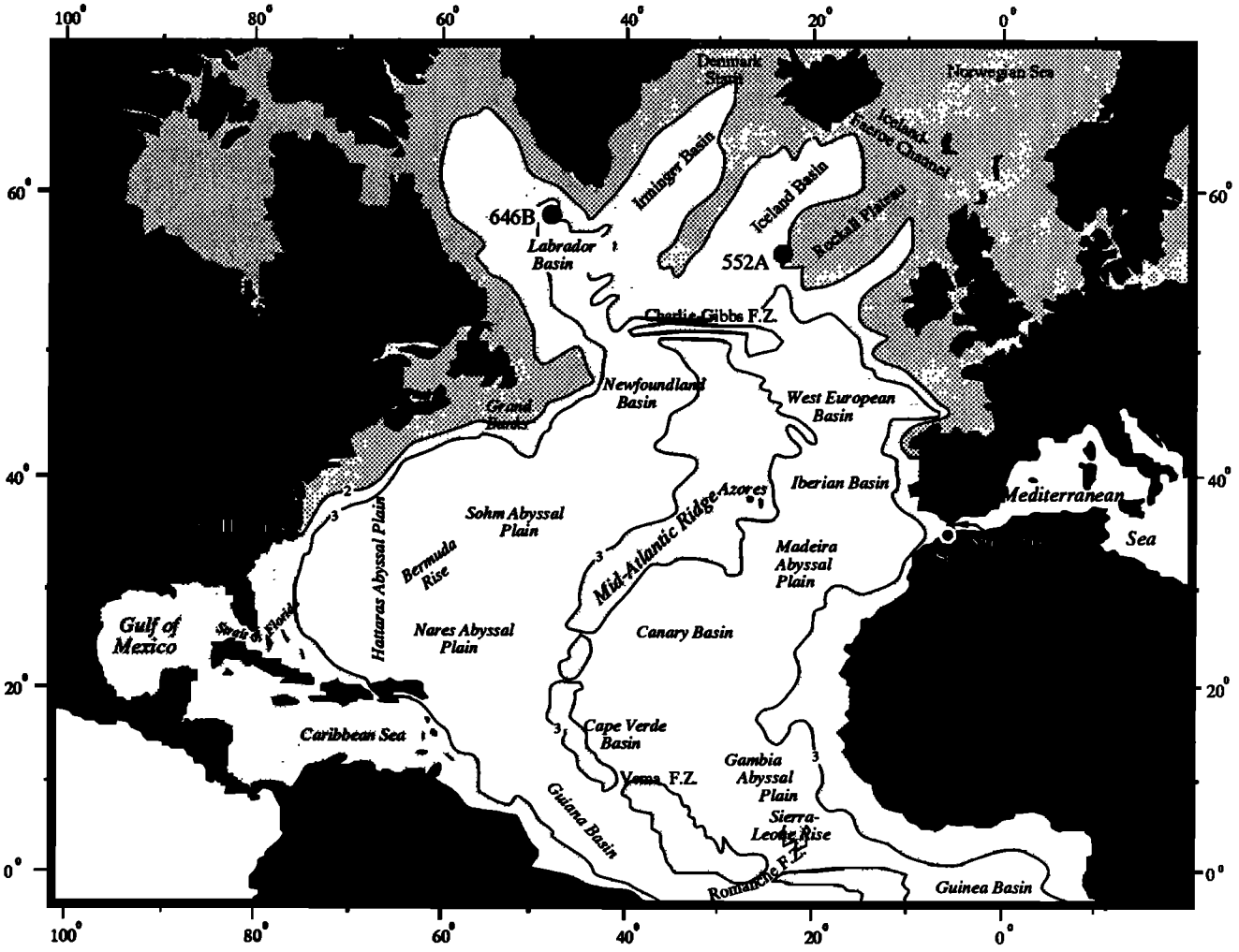

Figure 1. Locality of Ocean Drilling Program (ODP) Site 646B and Deep Sea Drilling Project (DSDP) Site 552A.

and planktonic foraminifera were studied in the fraction greater than 63 μm.

Strontium Isotopes

Sr isotope analyses were performed on more than 200 specimens of mixed calcareous benthic and planktonic foraminifera from the greater than 150 μm size fraction, which were dissolved in 1.5 N HCL. Standard ion exchange techniques [*Miller et al.*, 1991] were used to separate strontium for analyses on a VG Sector mass spectrometer at Rutgers University, New Jersey, USA. Internal precision (interrun variability) is approximately ±0.000008 (mean 2σ error) [*Miller et al.*, 1991]; external precision (interrun variability) is approximately ±0.000024 or better [see *Miller et al.*, 1991; *Oslick et al.*, 1994]. At Rutgers, NBS 987 is routinely measured as 0.710252 (2σ standard deviation 0.000026; n = 35) [*Miller et al.*, 1991] normalized to $^{87}Sr/^{86}Sr$ of 0.1194. *Farrell et al.* [1995] estimated that the rate of increase of $^{87}Sr/^{86}Sr$ (from 4.8 Ma to 7.0 Ma) was ~0.00005/m.y. Sr-isotope age estimates were determined using these equations calculated from the regression of *Farrell et al.* [1995]:

Age = 59941.95 - (Sr 87/86) x 84530.85 (Sr = 0.709080 - 0.709056).

for 2.5 - 4.8 Ma (K.G. Miller, written communication with J.W. Farrell, 1995), based on *Farrell et al.*'s data [1995].

Age = 15640.06 - (Sr 87/86) x 22050.72 (Sr = 0.709056 - 0.708955).

for 4.8 - 7.3 Ma (K.G. Miller, written communication with J.W. Farrell, 1995), based on *Farrell et al.*'s data [1995].

Oxygen and Carbon Isotopes

Oxygen and carbon isotopic data are from *Aksu and Hillaire-Marcel* [1989] (Site 646B) and *Keigwin* [1987] (Site 552A).

Results

Faunal and Floral Distribution

Ninety samples from Cores 40-80 (389-789 m subbottom depth (msb); core recovery 37.1% in average) [*Srivastava et al.*, 1989a, b] were studied for benthic foraminifera, yielding a sample spacing two to five samples per core depending on recovery. Over 100 species have been identified (Appendix 1[1]). The number of benthic foraminifera per cubic centimeter is rather consistent throughout the hole but increases slightly downward (Figure 2) and decreases sharply in the Tortonian section. The systematic taxonomy for the benthic foraminiferal species is given in Table 1.

[1] An electronic supplement of this material may be obtained on a diskette or Anonymous FTP from KOSMOS.AGU.ORG. (LOGIN to AGU's FTP account using ANONYMOUS as the username and GUEST as the password. Go to the right directory by typing CD APEND. Type LS to see what files are available. Type GET and the name of the file to get it. Finally, type EXIT to leave the system. (Paper 96PA00572, Messinian deep-water turbidites and glacioeustatic sea-level changes in the North Atlantic: Linkage to the Mediterranean Salinity Crisis, Jijun Zhang and David B. Scott). Diskette may be ordered from American Geophysical Union, 2000 Florida Avenue, N.W., Washington, D.C. 20009; $15.00. Payment must accompany order.

The Messinian (Cores 45X to 77X) is dominated by agglutinated foraminifera, while calcareous foraminifera dominate the Pliocene and Tortonian. Benthic/planktonic foraminiferal ratios are usually high in the Messinian section (Figure 2) and low during the Pliocene and Tortonian. Both calcareous/agglutinated and benthic/planktonic ratios exhibit high-amplitude variations.

Three small, brown marsh-type agglutinated benthic foraminiferal species, well known from marsh or coastal environments today [*Scott and Medioli*, 1980], are *Trochammina* cf. *squamata* (Figure 3, numbers 8 and 9), *Ammotium* sp. A (Figure 3, numbers 10-12), and *Miliammina fusca* (Figure 3, numbers 13 and 14). *Ammotium* sp. A occurs in most samples from Cores 42X-1 to 65X-CC, with the highest peak (15%) in Core 57X-3. It is rare below Core 65X (Figure 4). *Miliammina fusca* is found in Sample 63X-CC, 10-14 cm. *Trochammina* cf. *squamata* varies in abundance (Figure 2) at a high amplitude. These marsh forms are concentrated in nine levels, separated by layers accompanied with a relatively low proportion of shallow-water fauna (Figure 2). We suggest that the marsh foraminifera occur in turbidite layers, together with plant seeds, oxidized plant fragments, rounded quartz, highly polished benthic foraminiferal shells, wood fragments, pyrite-filled foraminiferal shells, highly concentrated mica, and gypsum crystals.

Deep-water agglutinated foraminifera, such as *Rhizammina* spp., *Psammosphaera* spp., and *Lagenammina* spp., are common from Samples 42X-7 to 51X-1, from 55X-2 to 63X-CC, and from 65X-7 to 68X-4 but are absent or extremely rare from Core 69X-1 to Core 80X-2 (Figure 4). Other deep-water agglutinated foraminifera, such as *Martinotiella communis, Cyclammina cancellata*, and *Recurvoides* spp., occur sporadically.

The most abundant occurrence of deep-water calcareous foraminifera is in the Tortonian and lower Pliocene (below Core 77X and above Core 43X). Calcareous faunas are dominated by nonionids (including *Pullenia bulloides, P. quinqueloba, Melonis barleeanum,* 0 to 30%) (Figures 5 and 6), *Eponides weddellensis* (0-25%), *Oridorsalis umbonatus* (0 to 10%), *Eponides tumidulus* (0-7%), and *Gyroidina* spp. (0-5%), with considerable variation. *Epistominella exigua* and *Nuttallides umbonifera* are extremely low in abundance, usually less than 2% in the Messinian. *N. umbonifera* is most common (~3-6%) near seismic reflector R3 (680.48-703.8 msb; Cores 72X-1 to 74X-4), similar to that reported by *Kaminski et al.* [1989] (~20-80%), but much lower. This probably resulted from the different size fraction of benthic foraminifera examined in this study (>63 μm) and that in Kaminski et al.'s study (>125 μm). The fraction of >125 μm does not contain numerous small-sized benthic foraminifera, the major component of the total benthic community; *E. exigua* reaches a peak of 23.3% in the Tortonian (Figure 5). These bathyal calcareous foraminifera separate the intervals with marsh foraminiferal layers in the Messinian. *Melonis barleeanum*, a typical form in glacial sediments in lower bathyal DSDP sites in northern Atlantic [*Murray*, 1984] and the Norwegian-Greenland Sea [*Talwani et al.*, 1976], is common from Cores 41X-2 to 50X-3. It is rare in Cores 53X-55X and almost absent from Cores 56 to 80 (Figure 6). Another calcareous deep-water species, *Cornuspirella diffusa*, is found up to ~20% in the Tortonian but is absent in the upper Messinian (Figure 4).

Deep-Water Turbidite Deposits

Deep-water turbidites are characterized by marsh foraminifera and terrigenous deposits and occur in nine discrete layers throughout the Messinian and lower part of the Pliocene at Site 646B (see Figure 2 for details).

Table 1. Systematic Taxonomy for Benthic Foraminiferal Species in Text

Species	References
Ammotium sp. A	Figure 3, numbers 10-12 [This paper]
Cornuspirella diffusa (Heron-Allen and Earland)	Figure 3, number 4 [This paper]
Cornuspira diffusa	*Heron-Allen and Earland* [1913, p. 272]
Cornuspirella diffusa (Heron-Allen and Earland)	*Loeblich and Tappan* [1988, p. 310, 311, Plate 323, Figure 1]
Cyclammina cancellata Brady	
Cyclammina cancellata	*Brady* [1884, p. 351, Plate 37, Figures 8-16]
Epistominella exigua (Brady)	
Pulvinulina exigua	*Brady* [1884, p. 696, Plate 103, Figures 13 and 14]
Pseudoparrella exigua (Brady)	*Phleger and Parker* [1951, p. 28, Plate 15, Figures 6 and 7]
Epistominella exigua (Brady)	*Hermelin and Scott* [1985, p. 208, Plate 4, Figure 6]
Eponides tumidulus (Brady)	
Truncatulina tumidula	*Brady* [1884, p. 666, Plate 95, Figures 8a-d]
Eponides tumidulus (Brady)	*Phleger and Parker* [1951, p. 21, 23, Plate 11, Figures. 7 and 8]
Eponides weddellensis Earland	
Eponides weddellensis	*Earland* [1936, p. 57, Plate 1, Figures. 65-67]
Globobulimina auriculata (Bailey)	
Bulimina auriculata	*Bailey* [1851, p. 12, Plate 1, Figures 25-27]
Globobulimina auriculata (Bailey)	*Thomas et al.* [1990, P. 227, Plate 6, Figures 3 and 4]
Globocassidulina subglobosa (Brady)	Figure 3, number 7 [This paper]
Cassidulina subglobosa	*Brady* [1881, p. 60]
Cassidulina subglobosa Brady	*Phleger and Parker* [1951, p. 27, Plate 14, Figures 11-13]
Globocassidulina subglobosa (Brady)	*Wang et al.*, 1988, p. 173, Plate 30, Figures 1 and 2]
Gyroidina soldanii (d'Orbigny)	
Rotalia soldanii	*d'Orbigny* [1826, p. 278, Figure 36]
Gyroidina soldanii (d'Orbigny)	*Hermelin and Scott* [1985, p. 210, Plate 5, Figures 6 and 8]
Martinottiella communis (d'Orbigny)	
Clavulina communis	*d'Orbigny* [1826, p. 268]
Martinottiella communis (d'Orbigny)	*Loeblich and Tappan* [1988, p. 171, Plate 190, Figures 3-4]
Melonis barleeanum (Williamson)	
Nonionina barleeana	*Williamson* [1858, p. 32, Plate 4, Figures 68 and 69]
Melonis barleeanum (Williamson)	*Wang et al.* [1988, p. 179, Plate 12, Figure 4]
Melonis pompilioides (Fichtel and Moll)	Figure 3, numbers 2 [This paper]
Nautilus pompilioides	*von Fichtel and Moll* [1798, p. 31, Plate 2, Figures a-c]
Melonis pompilioides (Fichtel and Moll)	*Hermelin and Scott* [1985, p. 212, Plate 6, Figure 5]
Miliammina fusca (Brady)	Figure 3, numbers 13 and 14 [This paper]
Quinqueloculina fusca	*Brady* [1870, p. 47, Plate 11, Figures 2 and 3]
Miliammina fusca (Brady)	*Scott et al.* [1991, p. 386, Plate 1, Figure 4]
Nuttallides umbonifera (Cushman)	Figure 3, number 3 [This paper]
Pulvinulinella umbonifera	*Cushman* [1933, p. 90, Plate 9, Figures 9a-c]
Nuttallides umbonifera (Cushman)	*Hermelin and Scott* [1985, p. 214, Plate 5, Figures 11 and 13]
Oridorsalis umbonatus (Reuss)	
Rotalina umbonata	*Reuss* [1851, p. 75, Plate 5, Figures 35a-c]
Oridorsalis umbonatus (Reuss)	*Hermelin and Scott* [1985, p. 214, Plate 5, Figure 10]
Planulina wuellerstorfi (Schwager)	Figure 3, number 5 [This paper]
Anomalina wuellerstorfi	*Schwager* [1866, p. 258, Plate 7, Figures 105 and 107]
Planulina wuellerstorfi (Schwager)	*van Morkhoven et al.* [1986, pp. 48-50, Plate 14, Figures 1-2]
Pullenia bulloides (d'Orbigny)	
Nonionina bulloides	*d'Orbigny* [1826, p. 293]
Nonionina bulloides	*d'Orbigny* [1846, p. 107, Plate 5, Figures 9 and10]
Pullenia bulloides (d'Orbigny)	*Wang et al.* [1988, p. 176, Plate 12, Figures 6 and 7]
Pullenia quinqueloba (Reuss)	
Nonionina quinqueloba	*Reuss* [1851, p. 71, Plate 5, Figure 31]
Pullenia quinqueloba (Reuss)	*Ujiie* [1990, p. 43, Plate 24, Figures 1-5]
Pyrgo murrhyna (Schwager)	Figure 3, number 6 [This paper]
Biloculina murrhyna	*Schwager* [1866, p. 203, Plate 4, Figures 15a-c]
Pyrgo murrhyna (Schwager)	*Ujiie* [1990, p. 16, Plate 4, Figures 3-5]
Rhizammina sp. A.	Figure 3, number 15 [This paper]
Trochammina cf. *squamata* Jones and Parker	Figure 3, numbers 8 and 9 [This paper]
Trochammina squamata	*Jones and Parker* [1860, p. 304]
Trochammina squamata Jones and Parker	*Wang et al.* [1988, p. 123, Plate 11, Figure 14]

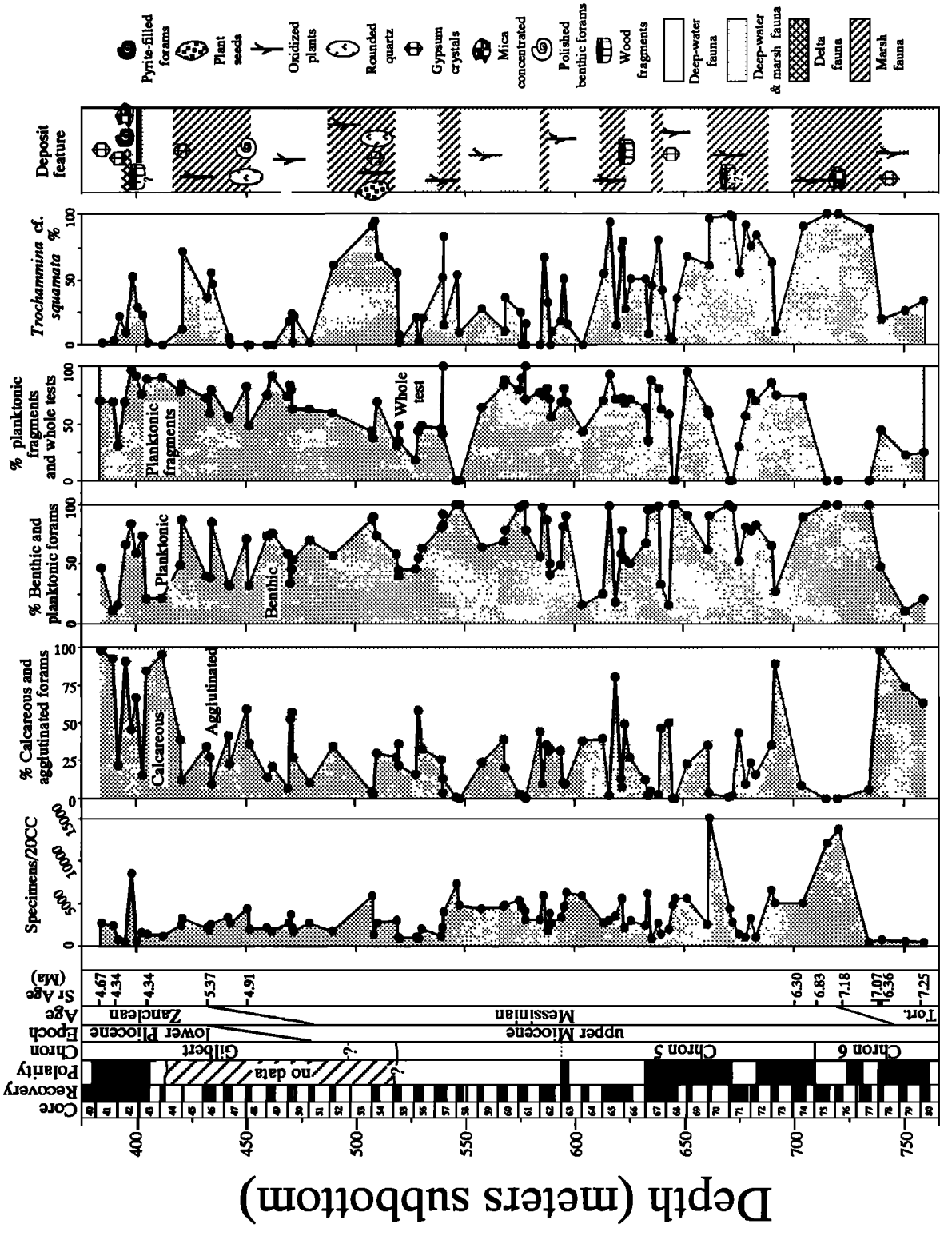

Figure 2. Distribution of benthic foraminifera from ODP Site 646B. The column to the right shows cyclic turbidites marked by marsh benthic foraminifera and other shallow water sediment components, interbedded with deep-water benthic foraminifera.

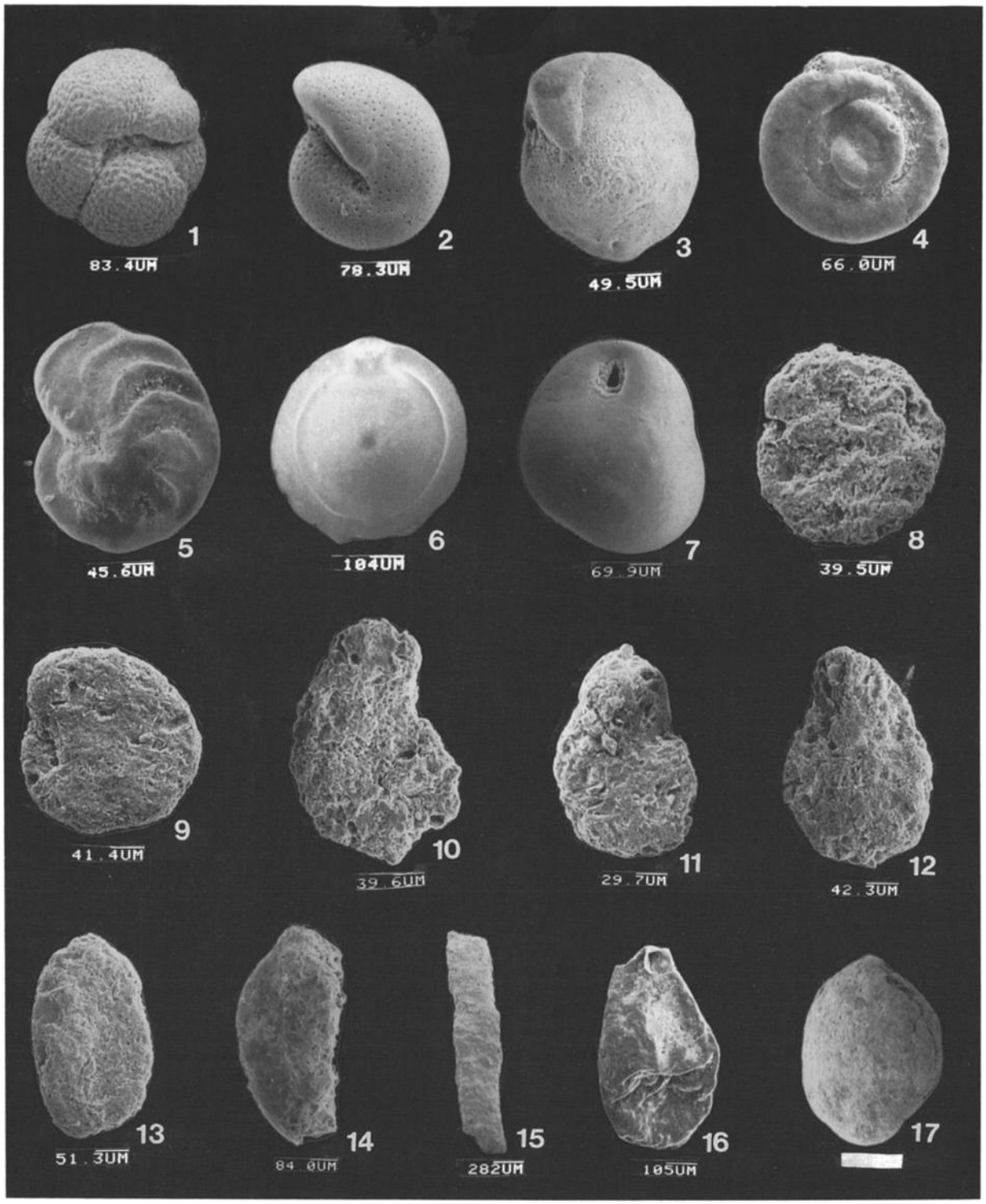

Figure 3. Benthic and planktonic foraminifera from ODP Site 646B. Numbers indicate the following: **1,** ***Neogloboquadrina atlantica,*** ventral view, from Site 646B, Core 44X-CC, 30-34 cm; **2,** ***Melonis pompilioides,*** side view, from Site 646B, Core 44X-CC, 30-34 cm; **3,** ***Nuttallides umbonifera,*** ventral view, from Site 646B, Core 44X-CC, 30-34 cm; **4,** ***Cornuspirella diffusa,*** side view, from Site 646B, Core 78X-CC, 26-30 cm; **5,** ***Planulina wuellerstorfi,*** ventral view, from Site 646B, Core 44X-CC, 30-34 cm; **6,** ***Pyrgo murrhyna,*** side view, from Site 646B, Core 44X-CC, 30-34 cm; **7,** ***Globocassidulina subglobosa,*** ventral view, from Site 646B, Core 44X-CC, 30-34 cm; **8** and **9,** ***Trochammina*** cf. ***squamata,*** ventral views, 8 from Site 646B, Core 69X-1, 40-44 cm, 9 from Site 646B, Core 75X-CC, 10-14 cm; **10-12,** ***Ammotium*** sp. A, side views, all from Site 646B, Core 76X-2, 50-54 cm; **13** and **14,** ***Miliammina fusca,*** side views, 13 from Site 646B, Core 69X-1, 40-44 cm, 14 from Site 646B, Core 76X-1, 100-104 cm; **15,** ***Rhizammina*** sp. A. side view, from Core 78X-CC, 26-30 cm; **16,** Plant fruit, from Core 71X-1, 5054 cm; **17,** Plant seed, from Core 54X-1, 140-144 cm.

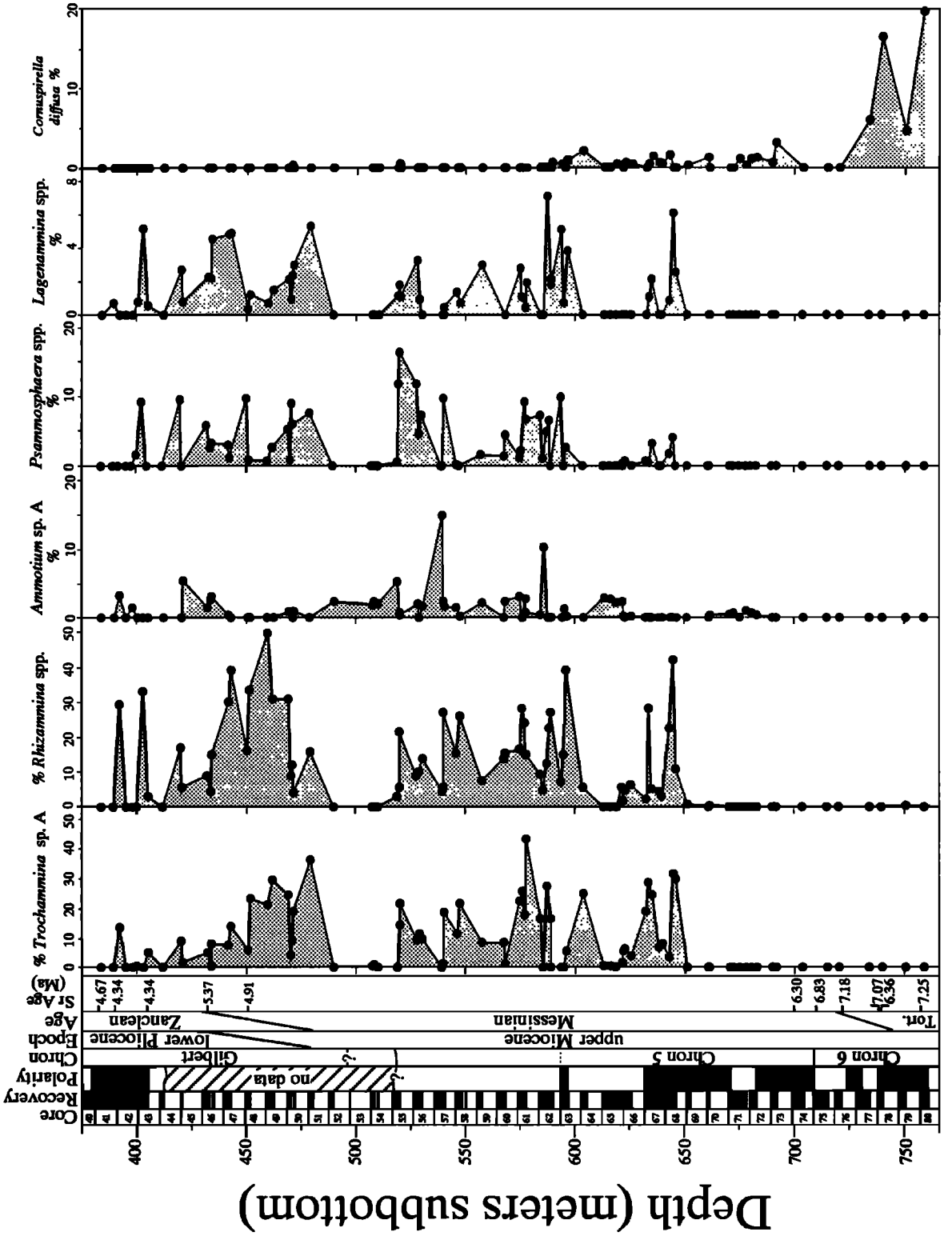

Figure 4. Distribution of deep-water calcareous benthic foraminifera from ODP Site 646B.

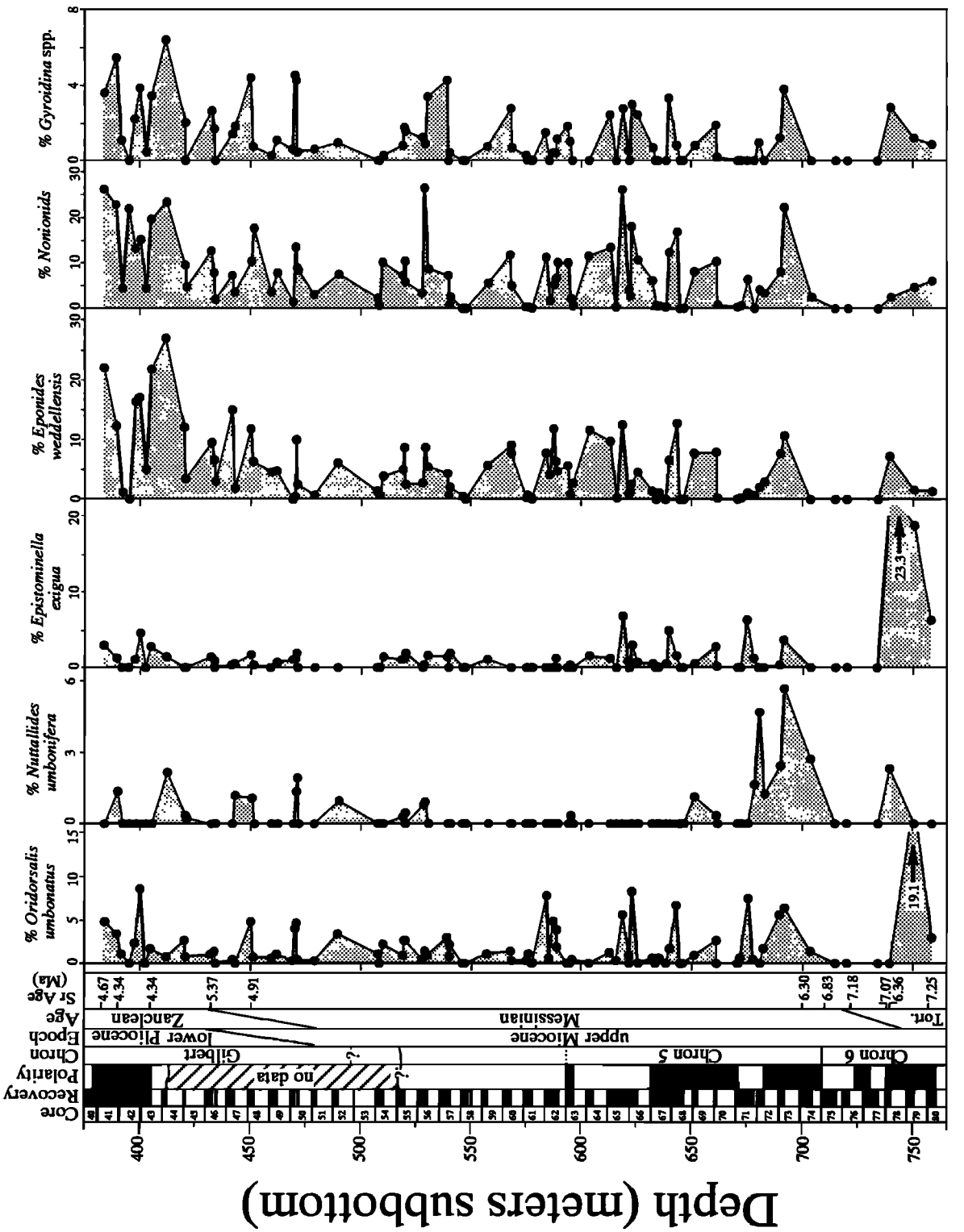

Figure 5. Distribution of deep-water agglutinated benthic foraminifera and *Cornuspirella diffusa* from ODP Site 646B.

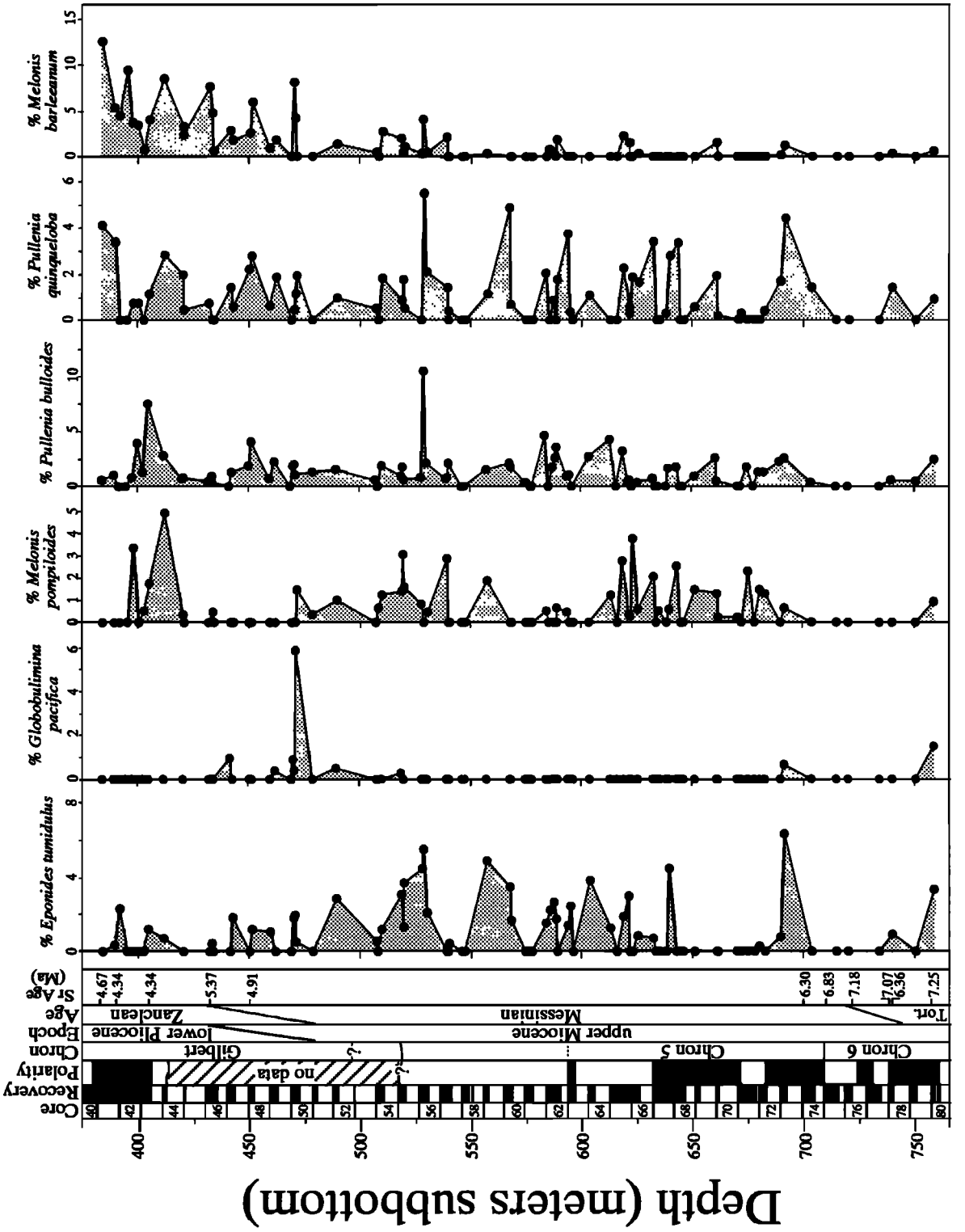

Figure 6. Distribution of deep-water calcareous benthic foraminifera from ODP Site 646B.

Pliocene turbidite cycle 1 (PTL 1) includes five samples (42X-1, 100-104 cm through 43X-2, 50-54 cm; 392 to 402.7 msb). Benthic foraminifera are relatively rare, dominated by small *Trochammina* cf. *squamata*, which ranges from 20% up to 53% of the total fauna. Calcareous foraminifera are small, thin-shelled, and filled with pyrite. This layer is composed of abundant mica and very fine, grey silts or clay, with gypsum crystals. The sediments represent typical deltaic deposits formed in an organic-rich environment. A few deep-water species are present (e.g., *Eponides weddellensis, Melonis barleeanum, Epistominella exigua*) at low percentages. These may have been mixed with the shallow-water forms during the downslope transport.

Layer 2 (i.e., Messinian turbidite cycle MTL 1) includes seven samples (45X-CC, 20-24 cm to 48X-1, 110-114 cm; 420.7 to 450.2 msb). This layer is dominated by *T.* cf. *squamata* (up to 55%) and *Ammotium* sp. A (up to ~5%). Oxidized plant fragments are common. Some highly rounded and polished quartz grains (>1 mm in diameter) and benthic foraminiferal shells occur at the base of the layer. All these indicate transport from a shallow organic-rich paleoenvironment. *Eponides weddellensis and Melonis barleeanum* are found in low percentages in this interval.

Layer 3 (MTL 2) contains five samples (52X-CC, 20-24 cm to 55X-2, 80-84 cm; 489.62 to 518.8 msb). This interval is dominated by *Trochammina* cf. *squamata* (70% to 95%) and about 2% *Ammotium* sp. A. Calcareous foraminifera occur at less than 1%. In Sample 54X-1, 140-144 cm, we also found an oxidized but well-preserved plant seed (Figure 3, number 17) and quartz grains (>1 mm in diameter). Oxidized grass/wood fragments are highly concentrated; these materials originated in a shallow-water, organic-rich paleoenvironment.

Layer 4 (MTL 3) includes four samples (57X-3, 40-44 cm; 57X-4, 22-26 cm; 57X-CC, 20-24 cm; and 58X-1, 50-54 cm; 539.2 to 546 msb). This layer is dominated by *T.* cf. *squamata* (~51% in average and maximum 83.6%), with a deep-water agglutinated form *Rhizammina* spp. (varying from 4% to 27%) and a few deep-water calcareous benthic foraminifera such as *Eponides weddellensis* and *Melonis barleeanum*.

In Layer 5 (MTL 4; 62X-2, 50-54 cm to 62X-3, 80-84 cm; 585.6 to 587.4 msb), *T.* cf. *squamata* is 66.8% in Sample 62X-2, 50-54 cm, and 27.3% in sample 62X-3, 80-84 cm. *Ammotium* sp. A reaches 10% in the former sample. Deep-water agglutinated and calcareous species include *Rhizammina* spp., *Psammosphaera* spp., *Lagenammina* spp., *Eponides weddellensis, Melonis barleeanum, Eponides tumidulus*, etc. Oxidized plant fragments are present.

Layer 6 (MTL 5) occupies the entire Core 65X (613.3 to 622.05 msb) and is characterized by marsh foraminifera, *T.* cf. *squamata* and *Ammotium* sp. A, with a maximum value of ~94%, with rare calcareous benthic foraminifera such as *Eponides weddellensis, Melonis* spp., *Oridorsalis umbonatus, Eponides tumidulus, Epistominella exigua, Gyroidina soldani*, etc. Oxidized plant fragments are common, and a large wood fragment (>1 cm long) occurs at the base of the layer.

Layer 7 (MTL 6) occurs in three samples in the lower part of Core 67X (67X-3, 40-44 cm, 67X-5, 50-54 cm, and 67X-6, 50-54 cm; from 635.2 msb to 639.8 msb). It is dominated by *T.* cf. *squamata*, varying from 41 to 81%. *Rhizammina* spp. is rare (4% on average). A deep-water *Trochammina* sp. is common (from 7 to 24%), and calcareous benthic foraminifera are rare. Oxidized plant fragments and gypsum crystals are present.

Layer 8 (MTL 7), from 661.55 msb to 682.71 msb, spans more than two cores (70X-CC, 20-24 cm to 72X-CC, 6-10 cm). Faunas are dominated by *T.* cf. *squamata*, with a maximum of 99%. *Ammotium* sp. A is rare, less than 1%. Wood fragments, oxidized grass/plant fragments, and plant fruit (Figure 3, number 16) are identified in this interval.

Layer 9 (MTL 8), from 703.8 msb to 734.1 msb (Cores 74X to 77X), is dominated by *T.* cf. *squamata*, which varies from 90% to 100%. Mica and oxidized grass/plant fragments are highly concentrated. Calcareous benthic and planktonic foraminifera are extremely rare.

Sr Stable Isotopes

Eleven samples were measured for strontium isotopes $^{87}Sr/^{86}Sr$ to determine the Tortonian/Messinian and Messinian/Pliocene boundaries (Table 2). Although the $^{87}Sr/^{86}Sr$ values are somewhat scattered, the values between 757.8 and 699.7 msb still show relatively constant increase upward at an average rate of 7.4×10^{-6}/10 m, similar to that from the Niue (8.5×10^{-6}/10 m) [*Aharon et al.*, 1993]. Two samples (78X-CC, 26-30 cm and 78X-2, 16-20 cm) exhibit values higher than adjacent ones. Our age estimates calculated from $^{87}Sr/^{86}Sr$ range from 7.25 Ma (Sample 80X-1, 80-84 cm) to 6.30 Ma (74X-1, 70-74 cm). Sample 76X-CC was dated at 7.18 Ma, very close to the age of Messinian/Tortonian boundary (7.12 Ma) based on the new timescale of *Berggren et al.* [1995].

The $^{87}Sr/^{86}Sr$ ratios from the interval between 450.9 and 384.1 msb (Core 48X-2 to 41X-2) vary from 0.709033 to 0.709062, with general increase upward, yielding ages ranging from 5.37 (with error ±0.15 Ma) to 4.34 Ma (with error ±0.42 Ma). In Sample 41X-2, 130-134, Sr exhibits a value of 0.709058 ± 0.000008. The anomalous Sr values are probably caused either by sample contamination or by downslope mass transportation. We prefer the latter interpretation.

Table 2. The $^{87}Sr/^{86}Sr$ Ratio and Age Calculation at Ocean Drilling Program Site 646B in the North Atlantic Ocean

Core	$^{87}Sr/^{86}Sr$	Error ±	Age, Ma	Age Error	Comments
41X-2	0.709058	0.000008	4.67	0.68	Age=59941.95-(Sr87/86X84530.85(Sr=0.709080-0.709056)
41X-6	0.709062	0.000005	4.34	0.42	Age=59941.95-(Sr87/86X84530.85(Sr=0.709080-0.709056)
43X-CC	0.709062	0.000005	4.34	0.42	Age=59941.95-(Sr87/86X84530.85(Sr=0.709080-0.709056)
46X-3	0.709033	0.000007	5.37	0.15	Age=15640.06-(Sr87/86)X22050.72(Sr=0.709056-0.708955)
48X-2	0.709054	0.000007	4.91	0.15	Age=15640.06-(Sr87/86)X22050.72(Sr=0.709056-0.708955)
74X-1	0.708991	0.000008	6.3	0.18	Age=15640.06-(Sr87/86)X22050.72(Sr=0.709056-0.708955)
75X-2	0.708967	0.000008	6.83	0.18	Age=15640.06-(Sr87/86)X22050.72(Sr=0.709056-0.708955)
76X-CC	0.708951	0.000008	7.18	0.18	Age=15640.06-(Sr87/86)X22050.72(Sr=0.709056-0.708955)
78X-2	0.708956	0.000044	7.07	0.97	Age=15640.06-(Sr87/86)X22050.72(Sr=0.709056-0.708955)
78X-CC	0.708988	0.000007	6.36	0.15	Age=15640.06-(Sr87/86)X22050.72(Sr=0.709056-0.708955)
80X-1	0.708948	0.000007	7.25	0.15	Age=15640.06-(Sr87/86)X22050.72(Sr=0.709056-0.708955)

Linear regression is from *Farrell et al.* [1995].

Stratigraphic Assessments

ODP Site 646B

Neither the Messinian/Tortonian nor the Messinian/Pliocene boundaries can be located precisely assigned due to the downslope transportation during the Messinian. We consider that the Messinian/Tortonian (M/T) boundary is between Cores 75X and 78X. This placement can be supported by the following observations (Figure 7):

1. The $^{87}Sr/^{86}Sr$ age estimate ranges from 7.07 to 7.18 Ma in Cores 77X and 76X (Table 1), a reasonable range in defining this boundary.

2. The Chron 6 $\delta^{13}C$ shift occurs in Core 75X [*Aksu and Hillaire-Marcel*, 1989]. At other sites, the Chron 6 $\delta^{13}C$ shift is slightly above the M/T boundary (see Site 552A).

3. There is an $\delta^{18}O$ enrichment in Core 77X.

4. There is a *Neogloboquadrina* coiling change from the dextral to sinistral in Core 77X (Figure 7). This change oc-

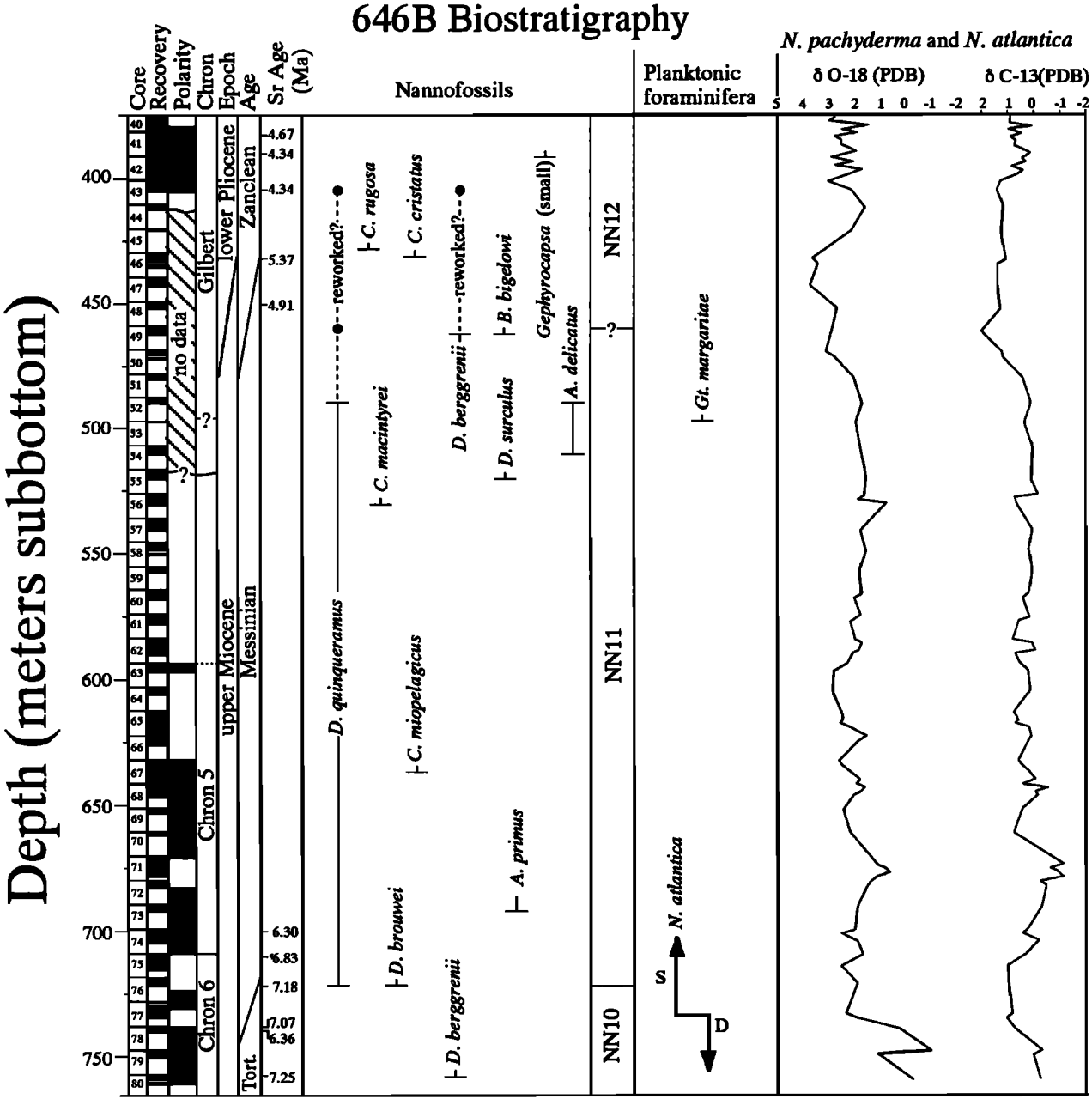

Figure 7. Messinian stratigraphy from ODP Site 646B from *Zhang* [1996]. Magnetostratigraphic chrons are reinterpreted after *Clement et al.* [1989]. Nannofossil data are from *Knüttel et al.* [1989]. Oxygen and carbon stable isotope are after *Aksu and Hillaire-Marcel* [1989]. T and reversed T represent first and last occurrences of nannofossils and planktonic foraminifera. Sr age estimates are from this study. D and S represent right and left coiling of *Neogloboquadrina atlantica*. The first occurrence of *Globorotalia margaritae* is from *Aksu and Kaminski* [1989]. PDB is pee dee belemnite.

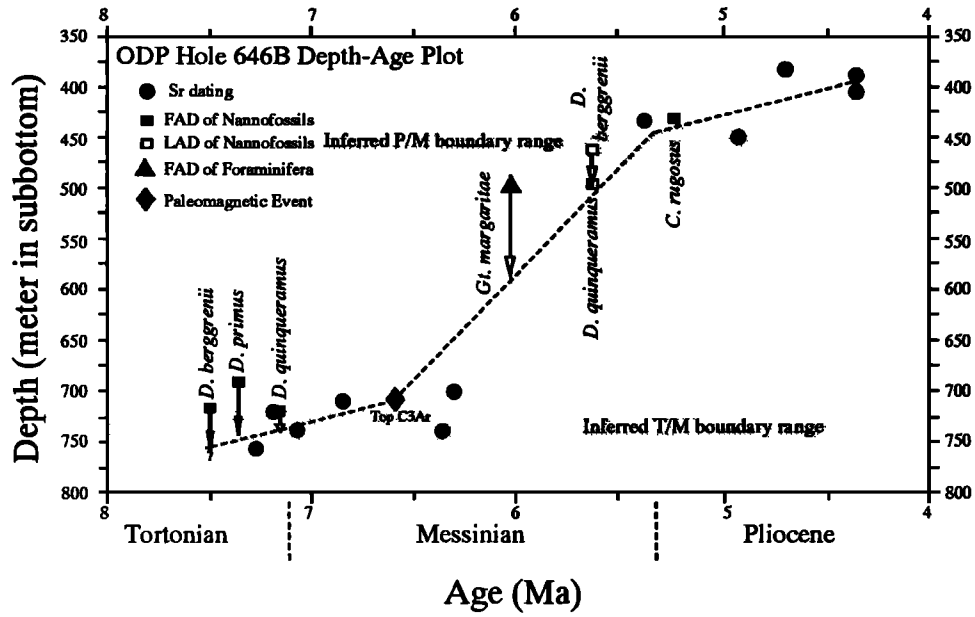

Figure 8. Depth-age plot of ODP Site 646B. Age estimates are from *Berggren et al.*[1995] and *Benson et al.* [1996] (see Table 3 for details). FAD is first appearance datum and LAD is last appearance datum. P/M is Pliocene/Miocene boundary.

curred immediately below the M/T boundary in Sites 552A and 608 and in the Moroccan Salé borehole [*Zhang*, 1996; *Zhang and Scott*, 1996].

5. The first occurrence (FO) of *D. berggrenii* occurred in Core 76X, which is obviously delayed (Figure 8; Table 3) as a result of downslope transportation [*Zhang*, 1996]. The FO of *Globorotalia conomiozea* marking the base of the Messinian is absent at this location.

The placement of the Messinian/Pliocene boundary is more difficult than that of the M/T boundary due to the scarcity of bioevents and poor core recovery from Core 43X to 53X (410 to 507 msb). We tentatively suggest that the Messinian/Pliocene boundary is between Cores 46X and 50X.

1. The last occurrence (LO) of *D. berggrenii* is in Sample 49X-CC. This event may be lower than the LO of *D. quinqueramus*, because the former is a zonal marker separating Subzones NN11a and NN11b [*Perch-Nielsen*, 1985].

2. The Sr age is 5.37 Ma (Sample 46X-3, 30-4 cm) with a value of 0.709033±0.0000007, while *McKenzie et al.* [1988] reported a mean $^{87}Sr/^{86}Sr$ value of 0.708995±0.00002 derived from five samples at the M/P boundary of the Capo Rossello stratotype. This difference may be related to the different lab performance because the interlab difference could have 15-30 ppm [K.G. Miller, personal communication, 1995]. *Farrell et al.* [1995] reported a $^{87}Sr/^{86}Sr$ ratio value of about 0.70904 at the M/P boundary from ODP Site 758, Indian Ocean using the

Table 3. Nannofossil, Paleomagnetic and Strontium Stable Isotopic Stratigraphic Events From ODP Site 646B

Events	Species	Core	Depth, msb	Age, Ma	References
	Sr	646B, 41X-2	384.1	4.67	
	Sr	646B, 41X-6	389.5	4.34	
	Sr	646B, 43X-CC	405.1	4.34	
FO	*C. rugosus*	646B, 46X-2	431.6	5.23	*Berggren et al.* [1995]
	Sr	646B, 46X-3	433.1	5.37	
	Sr	646B, 48X-2	450.9	4.91	
LO	*D. berggrenii*	646B, 49X-CC	461.9	5.6	*Berggren et al.* [1995]
FO	*Gt. margaritae*	646B, 52X-CC	497.0	6.0	*Berggren et al.* [1995]
LO	*D. quinqueramus*	646B, 53X-CC	497.2	5.6	*Berggren et al.* [1995]
FO	*D. primus*	646B, 73X-CC	692	7.35	*Benson et al.* [1996]
	Sr	646B, 74X-1	699.7	6.3	
Top	C3Ar	646B, 75X	708.6	6.567	*Berggren et al.* [1995]
	Sr	646B, 75X-2	711.1	6.83	
FO	*D. quinqueramus*	646B, 76X-CC	721.4	7.15	*Benson et al.* [1996]
	Sr	646B, 76X-CC	721.4	7.18	
	Sr	646B, 78-2	739.2	7.07	
	Sr	646B, 78X-CC	739.8	6.36	
	Sr	646B, 80X-1	757.8	7.25	
FO	*D. berggrenii*	646B, 80X-CC	716.0	7.48	*Benson et al.* [1996]

Age estimates of nannofossils are calibrated to the new timescale of *Berggren et al.* [1995] and *Benson et al.* [1996]. Nannofossil data are from *Knüttel et al.* [1989]. Paleomagnetic data are from *Clement et al.* [1989]. FO is first occurrence; LO is last occurrence.

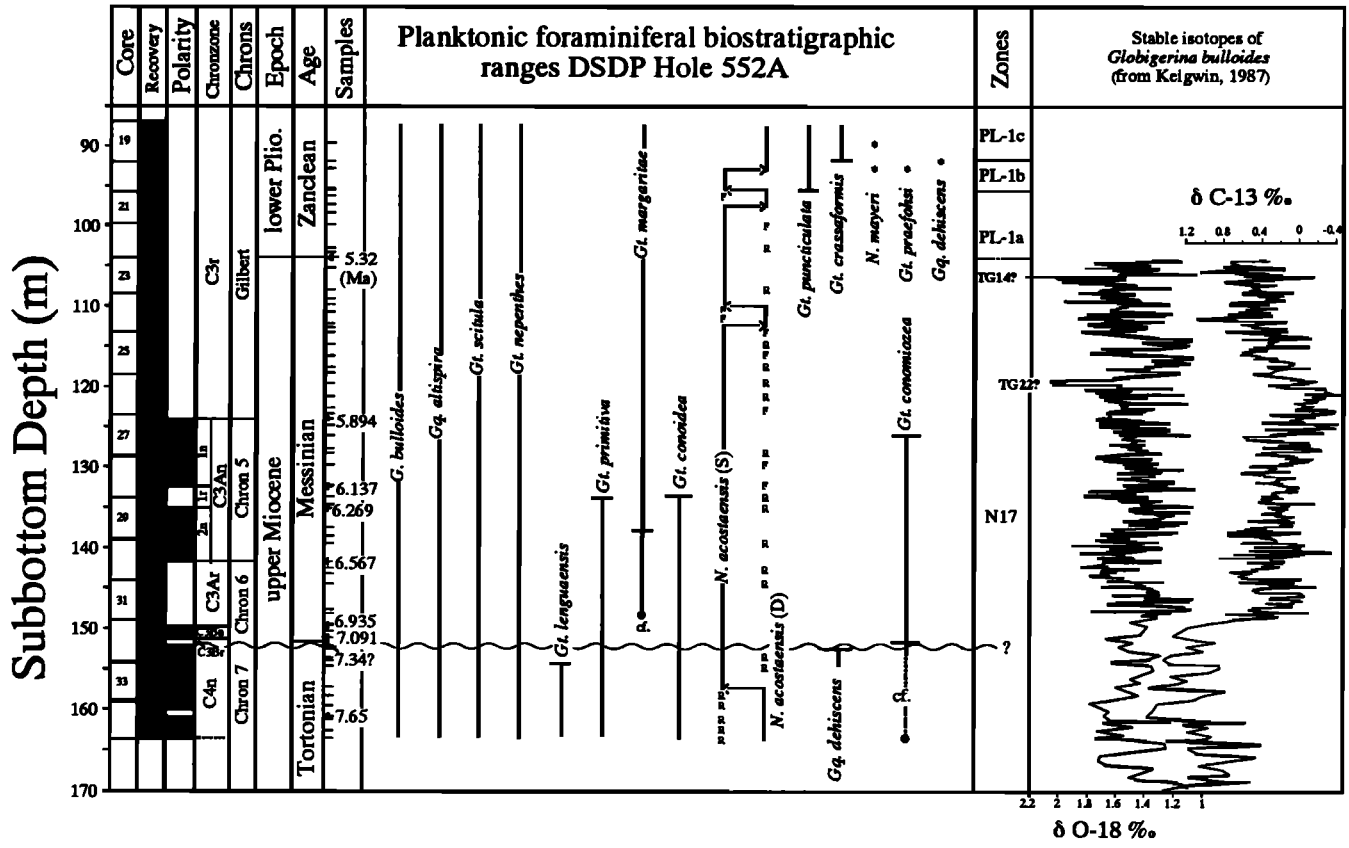

Figure 9. Messinian stratigraphy of DSDP Site 552A from *Zhang and Scott* [1996]. Paleomagnetic and oxygen and carbon stable isotope data are from *Keigwin* [1987]. "R" represents rare occurrence, and "F" indicates few occurrences. Asterisks indicate the intervals that are reworked or contaminated. Age estimates are from a new timescale of *Berggren et al.* [1995].

new timescale of *Berggren et al.* [1995]. Our $^{87}Sr/^{86}Sr$ is similar to that of *Farrell et al.* [1995].

3. The FO of *Gt. margaritae* (age estimate 6.0 Ma of *Berggren et al.* [1995]) is at 506.9 msb. and the FO of *Gt. puncticulata* (4.6 Ma of *Berggren et al.* [1995]) at 383.08 msb.

4. A $\delta^{18}O$ decrease occurs at depletion above Core 45X and a $\delta^{18}O$ increase from Cores 47X to 46X. These isotope events are basically identical to those observed in Sites 552A and 608 [*Zhang*, 1996; *Zhang and Scott*, 1996] and other locations in the world ocean [*Hodell et al.*, 1986]. Our boundary assignment is higher than those of *Knüttel et al.* [1989], *Baldauf et al.* [1989], and *Aksu and Kaminski* [1989], who placed the M/P boundary in Core 53X and 52X (Figure 7).

DSDP Site 552A

The Messinian/Tortonian boundary. The M/T boundary is recognized by the FO of *Globorotalia conomiozea* s.s. at 150.16 msb, the base of paleomagnetic Chronozone C3Bn (Figure 9; also see Table 4). The benthic $\delta^{13}C$ decrease of ~ 1‰ and a $\delta^{18}O$ increase of 0.5‰ occur at ~148 msb and the coiling direction change of *Neogloboquadrina acostaensis* at 154.62 msb, in the upper part of Chronozone C4n. The *Globorotalia* shift from *G. menardii* to *G. miotumida* observed in the Salé core (Morocco) [*Hodell et al.*, 1994a; *Benson et al.*, 1991] has not been determined by either *Huddlestun* [1984] or in this study, probably because the taxon is rare.

The Pliocene/Messinian boundary. This boundary is difficult to determine because no definite bioevents, magnetoevents, and chemo-events occur in this "quiet zone" (Figure 9). However, a relevant age estimate of the boundary may be interpolated through several pieces of indirect evidence:

1. The FO of *Gt. puncticulata* occurs in the lowermost Pliocene in temperate areas [*Berggren*, 1977; *Keller*, 1978, 1979a, b, c), and was used to define the PL1a and PL1b boundary. The FO of *Gt. crassaformis* denotes the PL1b/PL1c boundary [*Berggren et al.*, 1985], although it is absent, rare, or delayed in most low-latitude regions [*Keigwin*, 1982; *Thunell*, 1981; *Srinivasan and Chaturvedi*, 1992; *Berggren et al.*, 1995]. In spite of the current consideration that the FOs of the two species may be simultaneous in (sub)tropical regions [*Berggren et al.*, 1995], we recognized that *Gt. puncticulata* occurred prior to *Gt. crassaformis* (Figure 9), in agreement with *Huddlestun* [1984]. We calibrate the FO of *Gt. crassaformis* to 4.3 Ma and the FO of *Gt. puncticulata* to 4.6 Ma (see Table 4) based on the geomagnetic polarity timescale (GPTS) of *Berggren et al.* [1995]. We consider that the first occurrence of *Gt. puncticulata* denotes the lower Pliocene and that the P/M boundary must be below this level.

2. The TG14 oxygen isotope stage (see *Shackleton et al.* [1995] for TG definition) is at 106 msb and is estimated to be 4.8 Ma [*Keigwin*, 1987] that is now calibrated to ~5.55 Ma [*Berggren et al.*, 1995], below the P/M boundary [*Shackleton et al.*, 1995].

3. Using our age-depth plot (Figure 9), we interpolate the P/M boundary at 103 msb between the FO of *Gt. puncticulata* and TG14 isotope stage, in agreement with *Keigwin* [1987].

Table 4. Paleomagnetic, Oxygen Stable Isotopic and Biological Stratigraphic Events From DSDP Hole 552A

Sample	Events	Depth, msb	Age Estimates, Ma
19cc, 10-14	FO *Gt. crassaformis*	91.00	4.3*
27-1, 4-8	FO *Gt. puncticulata*	95.35	4.6*
	TG14	107.0	5.55
	TG22	119.0	5.75
27-2, 049	C3r base	124.44	5.894
28-3, 075	C3An.1r top	132.25	6.137
29-1, 099	C3An.1r base	134.49	6.269
29-3, 83-87	FO *Gt. margaritae*	137.33	6.0
30-3, 074	C3Ar top	141.98	6.567
32-1, 144	C3Ar base	149.94	6.935
32-2, 16-20	FO *Gt. conomiozea*	150.16	7.12
32-2, 144	C3Br top	151.44	7.091
32-3, 051	C3Br base	152.01	7.34
32-3, 94-98	LO *Gq. dehiscens*	152.4	5.8
33-1, 112-116	LO *Gt. lenguaensis*	154.62	6.0
34-2, 098	C4n.1r base	160.98	7.65

Age estimates of planktonic foraminiferal and paleomagnetic events are calibrated to the new timescale of *Berggren et al.* [1995]. Paleomagnetic data are from *Keigwin* [1987]. Oxygen isotopic age estimates are calibrated to *Shackleton et al.* [1995]. FO is first occurrence; LO is l ast occurrence.

* Age estimates are calibrated to the new timescale of *Berggren et al.* [1995] in this study.

Discussion

Origin of the Deep-Water Turbidites

Turbidites are usually recognized by graded bedding, sediment components, and tractional structures. Typical turbidite sequences are known as Bouma sequences, which consist of five divisions, A, B, C, D, and E, as function of grain size change from coarse (bottom) to fine (top). However, in the most cases, a complete Bouma sequence is not recorded, especially in distal sequences. From the micropaleontological point of view, all our turbidite layers are characterized by a well-stratified two-layer structure, a mixed faunal layer below, with a marsh faunal layer capping the sequence (Figure 2), thus suggesting a turbidite origin with the various turbidite packages separated by hemipelagic sediments that have a strictly deep-water fauna. The deep-water faunal layer has *Eponides weddellensis, Melonis* spp., *Gyroidina soldani, Uvigerina* spp., *Globocassidulina subglobosa, Pullenia bulloides,* etc., with extremely rare shallow water components; the mixed layer contains mainly deep-water fauna as given above, with lesser amounts of shallow water agglutinated forms such as *T.* cf. *squamata* and *Ammotium* sp. A., which may vary from 10% to 50%, and the marsh faunal assemblage is dominated by *T.* cf. *squamata* and *Ammotium* sp. A (60% to 100%). These repeated three-layer packages throughout the hole strongly suggest turbidite origin for the mixed and marsh foraminiferal layers. We suggest that the deep-water faunal layer is formed during high sea-level periods and the latter two are formed by downslope transportation from the subaerially exposed continental shelf edge off southwest Greenland, where the marsh foraminifera dwelled (Figure 10). Chaotic lithological textures in the interval bracketed by reflectors R2 and R3/4 (lithological Unit 3, now known as an equivalent to the Messinian) were confirmed by acoustic signals of multichannel seismic reflections reported by *Arthur et al.* [1989, Figure 9 of p. 967], suggesting the presence of turbidites during Messinian time.

It is difficult to determine exactly how many turbidite flows there are in each layer based on the homogenous sedimentary structure, log data, faunal compositions, and the poor core recovery. The turbidite layers vary considerably in thickness (recovered thicknesses ranging from 1 to 12 m). As distal phases of turbidites, their thicknesses suggest that each layer certainly contains numerous turbidite flows that formed during lower sea-level stands.

In ODP Site 646B, the typical Bouma sequence does not exist, because the sediment components are relatively homogenous and mainly composed of clay [*Srivastava et al.,* 1989a, part. 1, p. 488, Figure 54; *Srivastava et al.,* 1989b]. In Layer 2, coarser sediments such as polished quartz grains and rounded, large shallow-water benthic foraminiferal shells occur at the base of the layer, while finer components are at the top, indicating fining upward. Younger turbidites (early Pliocene) at this site have parallel- and cross-laminated siliciclastic silts, but those are attributed to traction transportation by vigorous bottom currents (contour currents) in the vicinity of Eirik Ridge [*Hiscott et al.,* 1989].

Significant changes at Site 646 in texture of the Messinian section were observed and considered to be related to an intensification of deep-water currents [*Cremer,* 1989]. Similar conclusions on the association with active deep-water circulation were also suggested by *Kaminski et al.* [1989] based on the presence of epibenthic suspension-feeders, *Rhizammina,* which strongly dominated in lithological Unit 3 (equivalent to the Messinian) at this site. *Wolf* [1991] also interpreted changes in benthic foraminifera from this site in terms of fluctuations in the intensity and composition of the Denmark Strait Overflow. Suspension feeding communities require gentle bottom currents to bring them food, and they may be common in the area of contour currents [*Schröder,* 1986]. However, when currents are too strong, these epifaunal tubular forms will be the first to be transported [*Kaminski et al.,* 1988a]. Concentrations of these forms (*Rhizammina*) also occur in laminated fine-grained turbidites [*Kaminski et al.,* 1988a]. Our benthic foraminiferal data show that *Rhizammina* is concentrated in mixed faunal layers, rather than in deep-water faunal layers which presumably formed in relatively stable environments during high sea-level stands. *Scott et al.* [1989] saw similar sequences in the Quaternary of Baffin Bay (site surveys for ODP Leg 105, Site 645), where there were turbidite layers, hemipelagic layers, and then a layer of sediments with only

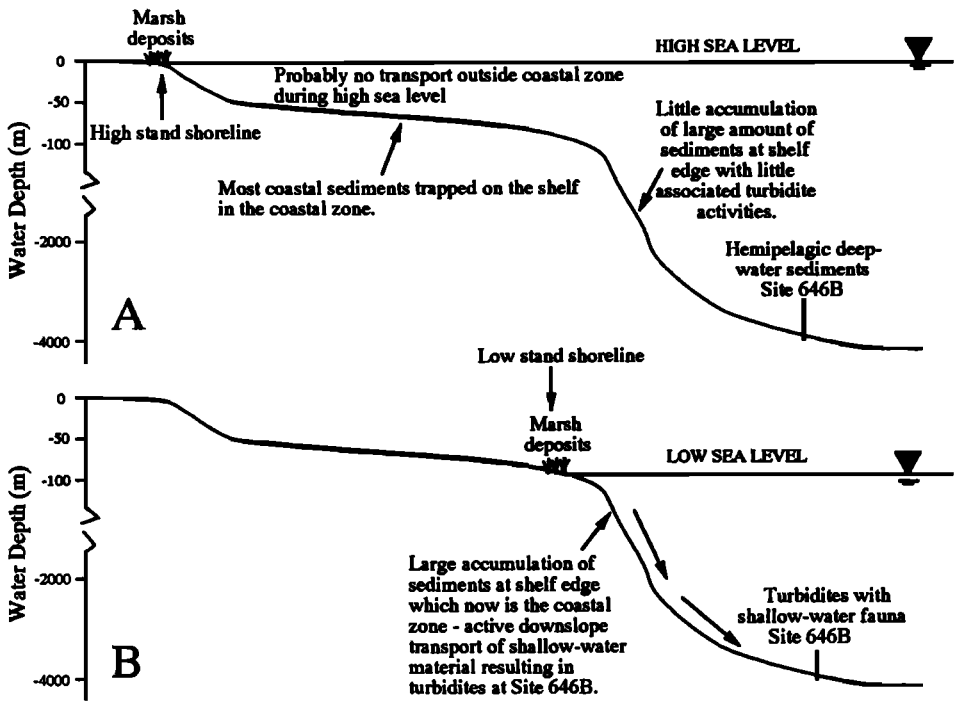

Figure 10. Schematic diagram of southern Greenland margin with both high and low stands of sea level and suggested sediment mechanisms for deep-sea turbidites at ODP Site 646B. (a) high sea-level stand; and (b) low sea-level stand.

Rhizammina algaeformis linings; this sequence repeated several times. The turbidites did not have marsh foraminifera, however, because the Quaternary turbidites were fed by glacial debris, not slumping of coastal deposits as we see at Site 646B in the Messinian. Thus we suggest the *Rhizammina* assemblage to be more likely an association with some downslope sediment transportation controlled by sea-level fluctuations through the submarine channel in the southwest of Greenland [*Arthur et al.*, 1989]. This transportation may provide sufficient food for the suspension feeders. We speculate that at Site 646B, the deep-water circulation may play a less important role in the occurrence of *Rhizammina*, the tubular forms which appear to characterize disturbed sites but display a poor ability to quickly recolonize substrate [*Kaminski et al.*, 1988b].

Correlation Between Turbidite Layers and Glacioeustatic Sea-Level Fluctuations

Maybe one of the most important aspects of the turbidites at Site 646B is their origin and the implication for sea level during the late Miocene. The foraminifera occurring in these turbidite layers are salt marsh foraminifera which have been demonstrated to have an extremely narrow range vertically (±10 cm) with respect to sea level and thus provide the most accurate means of relocating ancient sea level when found "in situ" [*Scott and Medioli*, 1978, 1980, 1986]. During high stands of sea level, carbon (and sediments) is trapped on the continental shelves and the coastal zone is remote to the shelf edge (Figure 10) if we assume a continental margin configuration for Greenland during the Messinian is similar to the present. Hence to have marginal marine foraminiferal fauna in turbidites, sea level must have been 80-100 m lower to expose the shelf edge to allow salt marsh formation near the edge [*Scott and Medioli*, 1986]. If sea level fluctuated between the present shoreline and the outer shelf as it does now off southern Greenland, then the presence of the marsh foraminifera in deep-sea turbidites during sea-level low stands suggests the amplitude of sea-level change to have been about 80-100 m. Although clearly the sea level was not at the present Quaternary shoreline in the Miocene, it is reasonable to assume there was a continental shelf in the Miocene with a similar morphology (i.e., wide platform) which when emerged rapidly would have had coastal deposits at the edge of the shelf with an 80-100 m sea-level lowering. This is why we think these data provide such an accurate measure of sea-level amplitude. In a similar setting in the Indian Ocean (ODP Leg 116, Site 717), there were many terrestrial plant fragments and some shallow-water foraminifera but never as many as at Site 646B [*Scott and Leger*, 1990] because sea level was probably not at the shelf edge at that location.

To understand the cause of the deep-water turbidite layers at Site 646B, we compare them with the oxygen isotopes of *Globigerina bulloides*, a surface water dweller, from DSDP Site 552A, where a complete, high-resolution oxygen isotope record for the Messinian interval has been obtained [*Keigwin*, 1987]. A smoothed $\delta^{18}O$ curve from the curve with three-point running average is plotted in Figure 11 against the turbidite layers from ODP Site 646B. This smoothed curve displays nine major episodes of $\delta^{18}O$ enrichment (Figure 11), which may correspond to the deep-water turbidite layers. Positive $\delta^{18}O$ excursions are proxies of cooling and sea-level lowering resulting from increase in the size of polar ice caps, which is in concert with the turbidite origin of an exposed Greenland shelf.

Using the late Quaternary $\delta^{18}O$ sea level calibration (0.11‰ $\delta^{18}O$ per 10 m of sea-level change [*Fairbanks and*

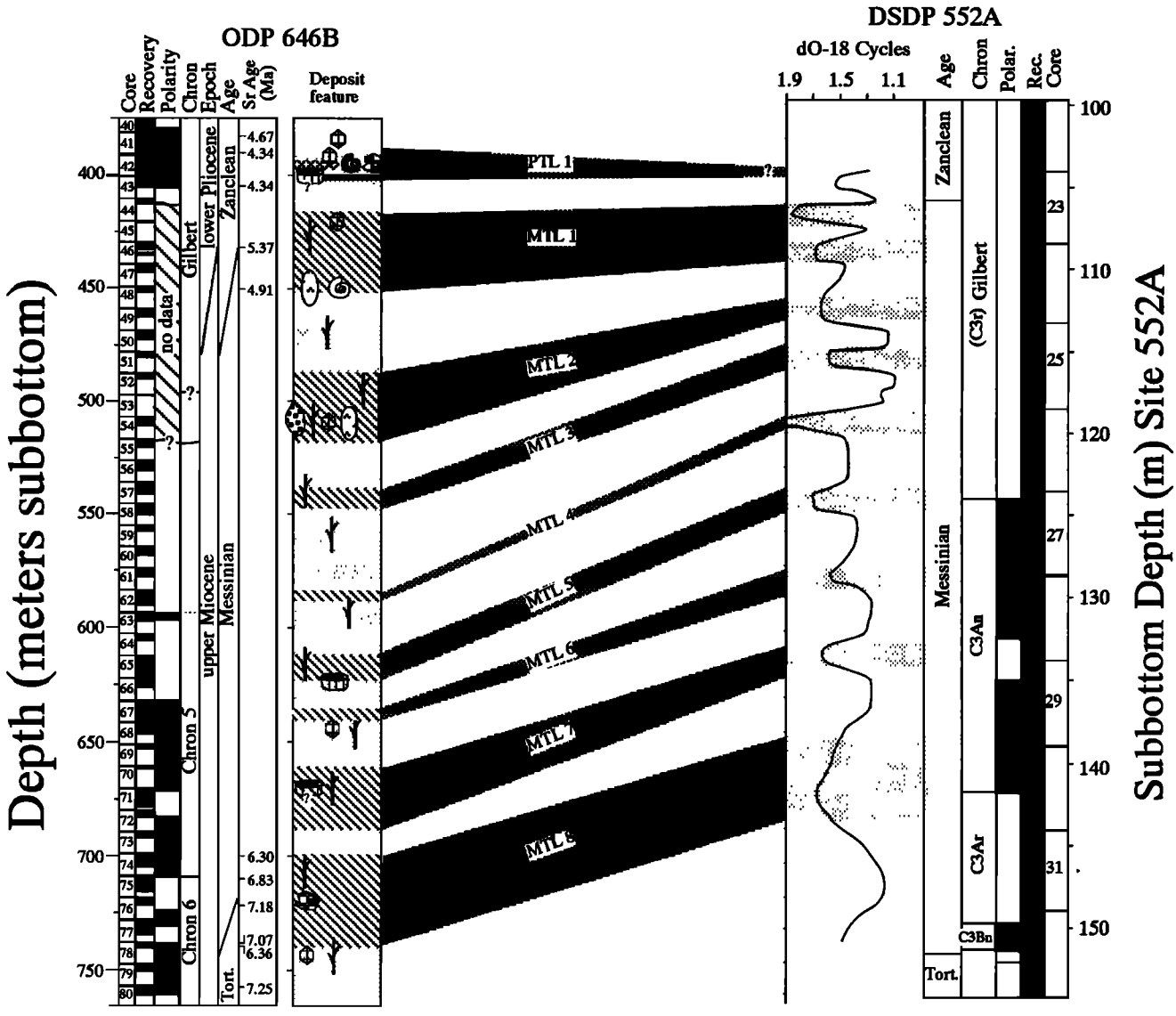

Figure 11. Correlation between the deep-water turbidite layers in Site 646B and oxygen stable isotope enrichment excursions at DSDP Site 552A. Oxygen stable isotopes from *Globigerina bulloides* were done by *Keigwin* [1987]. Smoothed $\delta^{18}O$ cycles were obtained from three-point running average curve based on the data given by *Keigwin* [1987]. MTL is Messinian turbidite layers. See Figure 2 for legends of lithologic section, ODP Site 646B.

Matthews, 1978; *Miller et al.*, 1987]), *Keigwin* [1987] suggested that a 0.6‰ benthic foraminiferal positive shift oxygen isotopes may correspond to 55 m sea-level lowering in the latest Miocene. He noted that this is a minimum estimate, because the unsmoothed $\delta^{18}O$ data show a 0.75 amplitude for the 5.55 Ma glacial event (4.8 Ma event of *Keigwin* [1987]), which would yield 68 m sea-level lowering. The amplitudes of other enriched benthic $\delta^{18}O$ peaks at Site 552A vary from 4 to 5.5‰ [*Keigwin*, 1987], suggesting 36-50 m sea-level lowerings. Similar estimates of late Miocene global sea-level lowering (40-70 m) were derived in southern Spain [*Berggren and Haq*, 1976], New Zealand [*Kennett*, 1967; *Roberts et al.*, 1994], Australia [*Carter*, 1978], the Pacific islands [*Adams et al.*, 1979], the Atlantic coastal plain of North America [*Adams et al.*, 1977], and the Mediterranean region [*Hsü et al.*, 1973a, b; *Cita and Ryan*, 1979; *McKenzie et al.*, 1979; *Müller and Hsü*, 1987; *Kastens and Mascle*, 1990]. *Aharon et al.* [1993] suggest a sea-level change of 10 m amplitude at the beginning of the Messinian, terminating in a large sea-level fall of at least 30 m near the Miocene/Pliocene boundary for Niue (South Pacific Ocean), rather different from these mentioned above. We consider that the amplitudes in Niue may have been coupled with covariation of tectonic uplifting and glacioeustatic fluctuations because Niue is located in an active tectonic region [*Cole and Lewis*, 1981; *Lincoln and Schlanger*, 1987]. This, however, remains uncertain because limited available tectonic data from this area [*Dubois et al.*, 1975] suggest a recent (Holocene) uplifting. Much evidence on ice volume growth at this time has been discovered worldwide both from land and ocean [*Mercer and Sutter*, 1982; *Shackleton and Kennett*, 1975; *Loutit and Kennett*, 1979; *Keigwin*, 1987; *Hayes et al.*,

1975; *Denton and Armstrong*, 1969; *Bandy et al.*, 1969; *McDougall et al.*, 1976; *Clark et al.*, 1980; *ODP Leg 151 Shipboard Scientific Party*, 1994; *Hodell et al.*, 1986, 1994b; *Kemp et al.*, 1975; *Ciesielski et al.*, 1982; *Pomar and Ward*, 1994].

On the basis of the marsh foraminifera at Site 646B, we suggest a substantially greater sea-level lowering from Site 646B data (80-100 m), which is more of a direct measurement based on certain assumptions (see Figure 10). The sea-level changes during the Messinian, unlike in any other periods of the Cenozoic, may have been controlled not only by ice volume changes but also by the repeated Mediterranean desiccation cycles. Atlantic water refilling into the Mediterranean Sea with an amount of 3.614×10^{15} m^3 could yield a global instantaneous sea-level lowering of about 10 m, according to the calculation of *Hsü et al.* [1977] and *Müller and Mueller* [1991], while a water transfer from the Mediterranean to global ocean area of 3.6×10^{14} m^2 could cause about 10 m sea-level rise and would be incorporated into the sea-level changes if a complete Mediterranean desiccation had taken place. On the basis of these considerations, we suggest that 80 m global sea-level lowering at least at 5.55 and 5.75 Ma is quite reasonable. It is obvious that there is an about 30 m difference in amplitude of sea-level changes between the estimates from marsh foraminifera at Site 646 and from $\delta^{18}O$ values at Site 552. The difference may be attributed to (1) an underestimation of amplitudes of Messinian $\delta^{18}O$ sea-level lowering because of water vapor evaporated from the Mediterranean Sea with lower $\delta^{18}O$ returning to the open ocean, which would result in a lower $\delta^{18}O$ value in the open ocean and possibly the cancellation of part of the ice volume signal; (2) tectonic difference from region to region; and (3) increasing area and altitude of growing ice sheets which lead to lower mean ice sheet $\delta^{18}O$ values [*Miller et al.*, 1987]. In this paper, we cannot assess the exact amplitudes of the global sea-level fluctuations during the Messinian but only those off Greenland. Sea-level fluctuations show great differences between regions, even in the Holocene [*Pirazzoli*, 1991].

Accurate chronology of the deep-water turbidites cannot be determined directly from our intra-Messinian stratigraphic data of ODP Site 646. The paleomagnetic data are not sufficiently reliable for precise dating because this interval proved less than satisfactory for magnetostratigraphic study due to poor recovery and drilling disturbance [*Clement et al.*, 1989]. However, if we assume the turbidites formed during climatic lowering of sea level, chronology of the turbidites can be suggested from our DSDP Site 552 depth-age plot (Figure 12), which indicates the climatic cycles from the smoothed $\delta^{18}O$ curve climax at 6.59, 6.22, 6.01, 5.89, 5.75, 5.7, 5.65, 5.60, 5.55, and 4.6 Ma, coeval with climate cooling (ice-volume) intervals. It should be pointed out that our calibrations cannot be correlated with 100k eccentricity from Site 552A given by *Beaufort and Aubry* [1990]. Because of the poor age control for the lower Gilbert paleomagnetic chron, we prefer the age estimates derived from the age-depth plot, rather than time series analysis. The nine oxygen excursions and deep-water turbidite layers could be coeval with eight unconformities in the Niue coral atoll east of Tonga Trench, South Pacific [*Aharon et al.*, 1993], which were formed during low sea-level stands during Messinian time. However, it is rather difficult to make detailed correlation between Site 646B turbidite layers and sea-level cycles from Niue of the Pacific Ocean [*Aharon et al.*, 1993] because they used 6.2 Ma as the Tortonian/Messinian boundary [*Berggren et al.*, 1985] and had poor stratigraphic control. At Site 646B, PTL 1 may be related to the early Pliocene glaciation at 4.6 Ma [*Burckle*, 1995].

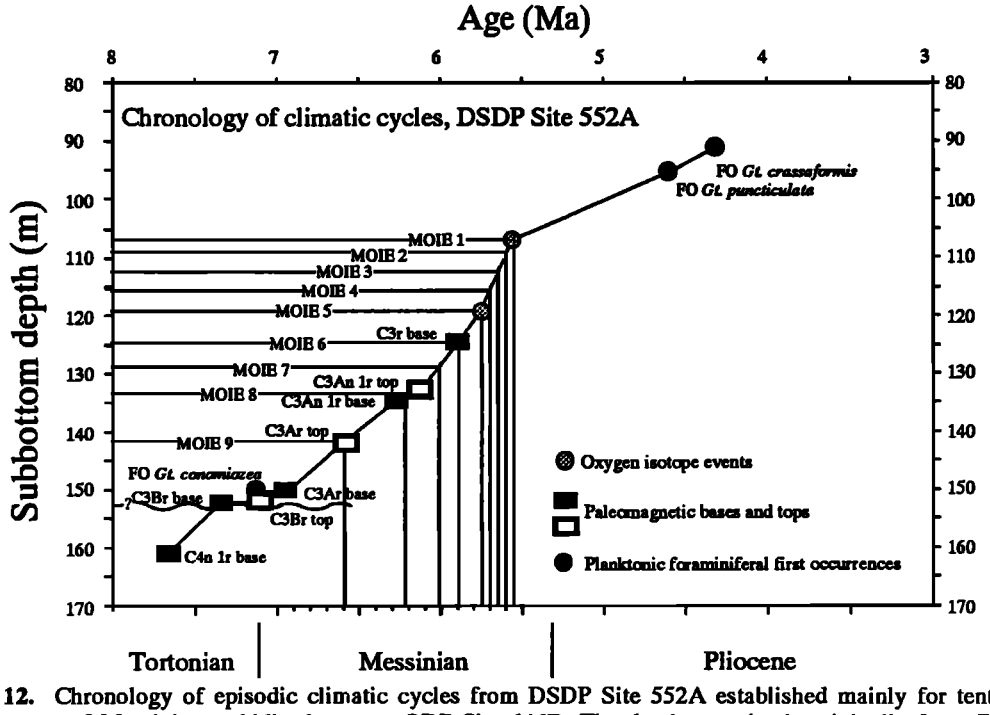

Figure 12. Chronology of episodic climatic cycles from DSDP Site 552A established mainly for tentative age estimates of Messinian turbidite layers at ODP Site 646B. The depth-age plot is originally from *Zhang* [1996]. MOIE is Messinian oxygen isotope enrichment. Paleomagnetic and oxygen stable isotope data are from *Keigwin* [1987].

Turbidite Layers and Sea-Level Changes Linked to the Messinian Salinity Crisis (5.9-5.32 Ma)

The Messinian sequence in the Mediterranean Basin is basically composed of five major successions, i.e., Tripoli marine formation, *Caliza Tosca* shallow-water deposits, Lower Evaporite, Upper Evaporite, and a thin layer of *Lago Mare* deposits (fresh/brackish water deposits) that capped the sequence. *Hsü et al.* [1973a, b], in their early work, claimed that to form a thickness of 2000-3000 m evaporites in the Mediterranean Sea, at least 11-13 inundations would be required if all salts were deposited in the center of the Mediterranean basin, or up to 100 inundations would be necessary if the salts were deposited evenly on the basin floor. *Benson and Rakic-El Bied* [1991] suggested seven to eight inundations, which is even less than Hsü's later suggestion (8-10 inundations) [*Benson and Rakic-El Bied* [1991]. These speculations greatly stimulated scientists to find connections between the isotope records in deep-sea marine sediments and the Mediterranean Messinian Salinity Crisis. So far, these have not been easily proven. Some authors remarked that two oxygen isotopic enrichment events may have corresponded to the Salinity Crisis, one in the youngest Chron 5 and the other in the earliest Gilbert, which have been linked to the formation of the Lower and Upper Evaporites in the Mediterranean Basin. [*McKenzie and Oberhänsli*, 1985; *Hodell et al.*, 1986; *Cita and McKenzie*, 1986; *Müller and Hsü*, 1987; *Keigwin*, 1987; *Zhang*, 1996]. Recently, the Messinian Salinity Crisis was correlated to eustatic changes indicated by eight unconformities from Niue coral atoll, South Pacific Ocean [*Aharon et al.*, 1993], but this requires further age recalibration for each unconformity.

Six oxygen enrichment excursions in the interval between 5.9 and 5.32 Ma are recognized (Figure 11), indicating more frequent climatic changes at this time than during the early Messinian (from 7.12 to 5.8 Ma). This interval is equivalent to the Messinian Salinity Crisis, caused by either limited Atlantic inflow or isolation of the Mediterranean from the Atlantic Ocean near 5.9 Ma as suggested by *Berggren et al.* [1995] (Note that *Gautier et al.* [1994] suggest a slightly later time, i.e., 5.8 Ma). The sea-level lowerings that led to the turbidite formation might also have contributed to the repeated isolation of the Mediterranean Basin during the late Messinian, although there are not as many as 11-13 inundations [*Hsü et al.*, 1973a, b] or seven to eight as suggested by *Benson and Rakic-El Bied* [1991]. We cannot expect the exact number of inundations in the Mediterranean to be recorded in deep-water turbidites suggested by *Hsü et al.* [1973a, b] or by *Benson and Rakic-El Bied* [1991], because of complicated geological/hydrological processes of deep-water turbidites and poor preservation and/or core recovery at Site 646B where part of the turbidite record could have been missing or not sampled.

Conclusions

Our benthic foraminiferal data clearly indicate that eight layers (MTL 1-8) of deep-water turbidites during the Messinian and one in the early Pliocene (PTL 1) formed at Site 646B (water depth 3461.3 m). These deep-water turbidite layers are characterized by high contents of agglutinated marsh benthic foraminifera (e.g., *Trochammina* cf. *squamata*, *Ammotium* sp. A, *Miliammina fusca*), rounded quartz, polished thick-shelled benthic foraminifera, wood fragments, plant seeds, fruits, and highly concentrated mica and are interbedded with sediments containing hemipelagic deep-water benthic faunas. These turbidites may be attributed to the distal turbidite facies because of the relatively homogenous clay components. A chronology for these deep-water turbidites has been tentatively correlated to the heavy $\delta^{18}O$ excursions at DSDP Site 552. The turbidite layers are dated at 6.59, 6.22, 6.01, 5.89, 5.75, 5.70, 5.65, 5.60, 5.55 and 4.6 Ma. The turbidites originated from intertidal deposits as indicated by their foraminiferal content, and they are the best direct measurement to define the amplitudes of sea-level lowering of 80-100 m during the Messinian. Sea-level falls could have been caused by increased polar ice volume, and/or by water transfer between the Mediterranean Sea and the Atlantic Ocean in the Messinian.

Our evidence suggests that the six deep-water turbidite layers during the late Messinian from ODP Site 646B and oxygen isotope excursions from DSDP Site 552A may be correlated to the Mediterranean Lower and Upper Evaporites, which might have formed if sea level lowered sufficiently to isolate partially or totally the Mediterranean Basin. The most profound climate changes occurred at 5.75 and 5.55 Ma, when the major bodies of the Lower and Upper Evaporites were formed. It is evident that the formation of Mediterranean evaporites has had a close affiliation with severe climate fluctuation during the Messinian.

Acknowledgments. The authors thank K.G. Miller and C. Liu for running Sr stable isotope from ODP Site 646B at Rutgers University, Piscataway, New Jersey, and L.D. Keigwin, at Woods Hole Oceanographic Institution, Massachusetts for providing us original stable isotope data from DSDP Site 552A. We also thank K.G. Miller for providing us part of the manuscript of Farrell et al. that is submitted to *Geology* and Lynne Maillet at the Department of Biology of Dalhousie University who helped us with the Scanning Electronic Microscope. C. Younger is acknowledged for her technical expertise in preparation of all the samples. Many thanks go to Kenneth G. Miller, Michael A. Kaminski, Richard H. Benson, and Ellen Thomas for their reviews of the manuscript. This work was supported by Izzak Walton Killam Memorial Scholarship at Dalhousie University to Jijun Zhang and partially supported by 1994 GSA Student Award and 1993 Cushman Foundation Student Award to Jijun Zhang, together with funds from a Natural Sciences and Engineering Research Council research grant to D.B. Scott.

References

Adams, C.G., R.H. Benson, R.B. Kidd, W.F.B. Ryan, and R.C. Wright, The Messinian Salinity Crisis and evidence of late Miocene eustatic changes in the world ocean, *Nature*, *269*, 383-386, 1977.

Adams, C.G., P. Rodda, and R.J. Kiteley, The extinction of the foraminiferal genus *Lepidocyclina* and the Miocene/Pliocene boundary problem in Fiji, *Mar. Micropaleontol.*, *4*, 319-339, 1979.

Aharon, P., S.L. Goldstein, C.W. Wheeler, and G. Jacobson, Sea-level events in the South Pacific linked with the Messinian salinity crisis, *Geology*, *21*, 771-775, 1993.

Aksu, A.E., and C. Hillaire-Marcel, Upper Miocene to Holocene oxygen and carbon isotopic stratigraphy of Sites 646 and 647, Labrador Sea, edited by S.P. Srivastava et al., *Proc. Ocean Drill. Program Sci. Results*, *105*, 689-695, 1989.

Aksu, A.E., and M.A. Kaminski, Neogene and Quaternary planktonic foraminifer biostratigraphy and biochronology in Baffin Bay and the Labrador Sea, edited by S.P. Srivastava et al., *Proc. Ocean Drill. Program Sci. Results*, *105*, 287-304, 1989.

Arthur, M.A., S.P. Srivastava, M. Kaminski, R. Jarrard, and J. Osler, Seismic stratigraphy and history of deep circulation and sediment drift development in Baffin Bay and Labrador Sea, edited by S.P. Srivastava et al., *Proc. Ocean Drill. Program Sci. Results*, *105*, 957-988, 1989.

Bailey, J. W., Microscopical examination of soundings made by the United States Coast Survey of the Atlantic coast of the United States, *Smithson. Contrib. Knowl.*, *2*, 1-15, 1851.

Baldauf, J.G. et al., Magnetostratigraphic and biostratigraphic synthesis of Ocean Drilling Program Leg 105: Labrador Sea and Baffin Bay, edited by S.P. Srivastava et al., *Proc. Ocean Drill. Program Sci. Results*, *105*, 935-956, 1989.

Bandy, O.L., E.A. Butler, and R.C. Wright, Alaskan upper Miocene glacial deposits and the *Turborotalia pachyderma* datum plane, *Science*, *166*, 607-609, 1969.

Beaufort, L., and M.-P. Aubry, Fluctuations in the composition of late Miocene calcareous nannofossil assemblages as a response to orbital forcing, *Paleoceanography, 5*(6), 845-866, 1990.

Bender, M.L., and L.D. Keigwin, Speculations about the upper Miocene change in abyssal Pacific dissolved bicarbonate $\delta^{13}C$, *Earth Planet. Sci. Lett., 45*, 383-393, 1979.

Benson, R.H., and K. Rakic-El Bied, Biodynamic, saline giant and late Miocene catastrophism, *Carbonates Evaporites, 6*(2), 127-168, 1991.

Benson R.H., K. Rakic-El Bied, and G. Bonaduce, An important current reversal (inflow) in the Rifian Corridor (Morocco) at the Tortonian-Messinian boundary: The end of Tethys Ocean, *Paleoceanography, 6*(1), 164-192, 1991.

Benson, R.H. et al., The Bou Regreg Section, Morocco: Proposed global boundary stratotype section and point of the Pliocene, *Notes Mem. Serv. Geol. Morocco, 383*, in press, 1996.

Berger, W. H., and V. Vincent, Deep-sea carbonates: Reading the carbon-isotope signal, *Geol. Rundsch., 75*, 249-269, 1986.

Berggren, W.A., Late Neogene planktonic foraminiferal biostratigraphy of DSDP Site 357 (Rio Grande Rise), edited by P.R. Supko et al., *Initial Rep. Deep Sea Drill. Proj., 29*, 591-614, 1977.

Berggren, W.A., and B. Haq, The Andalusian Stage (late Miocene): Biostratigraphy, biochronology and paleoecology, *Paleogeogr. Paleoclimatol. Paleoecol., 20*, 67-129, 1976.

Berggren, W.A., D.V. Kent, and J.A. Van Couvering, Neogene geochronology and chronostratigraphy, *The Chronology of the Geological Record.*, edited by N.J. Snelling, pp. 211-260, Blackwell Sci., Cambridge, Mass., 1985.

Berggren, W.A., D.V. Kent, C.C. Swisher III, and M.-P. Aubry, A revised Neogene geochronology and chronostratigraphy, in *Time Scales and Global Stratigraphic Correlations*, edited by W.A. Berggren et al., *Spec. Vol. Soc. Econ. Paleontol. Mineral. 54*, 129-212, 1995.

Brady, H. B., The ostracoda and foraminifera of tidal rivers, with analysis and descriptions of foraminifera, Part II, *Annu. Mag. Nat. His. Ser. 4, 6*, 273-309, 1870.

Brady, H. B., Notes on some of the reticularian Rhizopoda of the *Challenger* Expedition: Part 3. *Q. J. Microsc. Sci., New Ser., 2*, 31-71, 1881.

Brady, H. B., Report on the foraminifera dredged by the *H.M.S. Challenger* during the years 1873-1876, in *Report of the Scientific Results of the Exploration Voyage of H.M.S. Challenger, Zoology, 9*, 1-814, 1884.

Burckle, L., Overview of late Miocene/early Pliocene paleoclimate, Paper presented at the International Conference on the Biotic and Climatic Effects of the Messinian Event on the Circum-Mediterranean, Univ. Garyounis, Benghazi, Libya, 1995.

Carter, A.N., Phosphatic nodule beds in Victoria and the late Miocene-Pliocene eustatic event, *Nature, 276*, 258-259, 1978.

Ciesielski, P.F., M.T. Ledbetter, and B.B. Ellwood, The development of Antarctic glaciation and the Neogene paleoenvironment of the Maurice Ewing Bank, *Mar. Geol., 46*, 1-51, 1982.

Cita, M.B., and J.A. McKenzie, The terminal Miocene event, in *Mesozoic and Cenozoic Oceans*, Geodyn. Ser., vol. 15, edited by K.J. Hsü, pp. 123-140, AGU, 1986.

Cita, M.B., and W.B.F. Ryan, The Bou Regreg section of the Atlantic coast of Morocco: Evidence, timing and significance of a late Miocene regressive phase, *Riv. Ital. Paleontol. Stratigr., 84*, 1051-1082, 1978.

Cita, M.B., and W.B.F. Ryan, Late Neogene environmental evolution, *Initial Rep. Deep Sea Drill. Proj., 47*, 447-459, 1979.

Clark, D.L., R.R. Whitman, K.A. Morgan, and S.D. Mackey, Stratigraphic and glacial-marine sediments of the Amerasian Basin, central Arctic Ocean, *Spec. Pap. Geol. Soc. Am., 181*, 1-57, 1980.

Clement, B.M., F.J. Hall, and R.D. Jarrard, The magnetostratigraphy of Ocean Drilling Program Leg 105 sediments, edited by S.P. Srivastava et al., *Proc. Ocean Drill. Program Sci. Results, 105*, 583–595, 1989.

Cole, J.W., and K.B. Lewis, Evolution of the Taupo-Hikurangi subduction system, *Tectonophysics, 72*, 1-22, 1981.

Cremer, M., Texture and microstructure of Neogene-Quaternary sediments, ODP Sites 645 and 646, Baffin Bay and Labrador Sea, edited by S.P. Srivastava et al., *Proc. Ocean Drill. Program Sci. Results, 105*, 7-20, 1989.

Cushman, J. A., Some new Recent foraminifera from the tropical Pacific, *Contrib. Cushman Lab. Foraminifer. Res., 9*, 77-95, 1933.

Denton, G.H., and R.L. Armstrong, Miocene-Pliocene glaciations in southern Alaska, *Am. J. Sci., 267*, 1121-1142, 1969.

d'Orbigny, A. D., Tableau méthodique de la classees des céphalopods, *Ann. Sci. Nat., Ser. 1, 7*, 245-314, 1826.

d'Orbigny, A.D., *Foraminiferes Fossiles du Bassin Tertiaire de Vienne (Autriche): Classics in Paleontology*, no. 2, 321 pp + 17 plates, Gide et Comp^{e}, Paris, 1846.

Dubois, J., J. Launay, and J. Recy, Some new evidence on lithospheric bulges close to islands arcs, *Tectonophysics, 26*, 189-196, 1975.

Earland, A., Foraminifera, IV, Additional records from the Weddell Sea sector from material obtained by the S.Y. Scotia, *Discovery Rep., 13*, 1-76, 1936.

Fairbanks, R.G., and R.K. Matthews, The marine oxygen isotopic record in Pleistocene coral, Barbados, west Indies, *Quat. Res., 10*, 181-196, 1978.

Farrell, J.W., S.C. Clemens, and L.P. Gromet, Improved chronostratigraphic reference curve of late Neogene seawater $^{87}Sr/^{86}Sr$, *Geology , 23*, 403-406, 1995.

Gautier, F., G. Clauzon, J.-P. Suc, J. Cravatte, and D. Violanti, Age et durée de la crise de salinité messinienne, *C. R. Acad. Sci., séries II, 318*, 1103-1109, 1994.

Haq, B.U., T.R. Worsley, L.H. Burckle, R.G. Douglas, L.D. Keigwin, N.D. Opdyke, S.M. Savin, M.A. Sommer, E. Vincent, and F. Woodruff, Late Miocene marine carbon-isotopic shift and synchroneity of some phyoplanconic biostraigraphic events, *Geology, 8*, 427-431, 1980.

Hayes, D.E. et al., Sites 270, 271, 272, edited by D.E. Hayes et al., *Initial Rep. Deep Sea Drill. Proj., 28*, 221-234, 1975.

Hermelin, J.O.R., and D.B. Scott, Recent benthic foraminifera from the central North Atlantic, *Micropaleontology, 31*, 199-220, 1985.

Heron-Allen, E., and A. Earland, On some foraminifera from the North Sea, etc., dredged by the Fisheries Cruiser "Goldseeker" (International North Sea Investigations Scotland), III, On *Cornuspira diffusa*, a new type from the North Sea, *J. R. Microsc. Soci., Trans. and Proc.*, 272-276, 1913.

Hiscott, R.N., M. Cremer, and A.E. Aksu, Evidence from sedimentary structures for processes of sediment transport and deposition during post-Miocene time at Sites 645, 646 and 647, edited by S.P. Srivastava et al., *Proc. Ocean Drill. Program Sci. Results, 105*, 53-63, 1989.

Hodell, D.A., and J.P. Kennett, Late Miocene-early Pliocene stratigraphy and paleoceanography of the South Atlantic and Southwest Pacific oceans: A synthesis, *Paleoceanography, 1*(3), 285-311, 1986.

Hodell, D.A., K.M. Elstrom, and J.P. Kennett, Latest Miocene benthic O change, global ice volume, sea level, and the "Messinian Salinity Crisis", *Nature, 320*, 411-414, 1986.

Hodell, D.A., R.H. Benson, J.P. Kennett, and K. Rakic-El Bied, Stable isotope stratigraphy of late Miocene-early Pliocene sequences in Northwest Morocco: The Bou Regreg Section, *Paleoceanography, 4*(4), 467-482, 1989.

Hodell, D. A., R.H. Benson, D.K. Kent, A. Boersma, and K. Rakic-El Bied, Magnetostratigraphic, biostratigraphic, and stable isotope stratigraphy of an upper Miocene drill core from the Salé Briqueterie (northwestern Morocco): A high-resolution chronology for the Messinian Stage, *Paleoceanography, 9*(6), 835-855, 1994a.

Hodell, D. A., D.W. Müller, P. F. Ciesielski, and G.A. Mead, Synthesis of oxygen and carbon isotopic results from Site 704: Implication for major climatic-geochemical transitions during the late Neogene, edited by P.F. Ciesielski, et al., *Proc. Ocean Drill. Program Sci. Results, 114*, 475-480, 1994b.

Hsü, K.J., The desiccated deep-basin model for the Messinian events, in *Messinian Events in the Mediterranean*, edited by C.W. Drooger et al., *Geodyn. Sci. Rep.* , pp. 60-67, North-Holland Publishing, New York, 1973.

Hsü, K.J., The desiccation of the Mediterranean Sea, *Endeavour New Ser. 11*, 67-72, 1987.

Hsü, K.J., Mediterranean model: Posterity will judge, *Geotimes, 5*, Sept., 1988.

Hsü, K.J., M.B. Cita, and W.B.F. Ryan, The origin of the Mediterranean evaporites, edited by W.B. Ryan et al., *Initial Rep. Deep Sea Drill. Proj., 13*, 1203-1231, 1973a.

Hsü, K.J., W.B.F. Ryan, and M.B. Cita, Late Miocene desiccation of the Mediterranean, *Nature, 242*, 240-244, 1973b.

Hsü, K.J., L. Montadert, D. Bernoulli, M. B. Cita, A. Erickson, R. E. Garrison, R. B. Kidd, F. Milleres, C. Müller, and R. Wright, History of the Mediterranean salinity crisis, *Nature, 267*, 399-403, 1977.

Hsü, K.J. et al., *Initial Reports of the Deep Sea Drilling Project 42A*, 1249 pp., U.S. Gov. Print. Off., Washington, D.C., 1978.

Huddlestun, P.F., Planktonic foraminiferal biostratigraphy, Deep Sea Drilling Project Leg 81, edited by D.G. Roberts et al., *Initial Rep. Deep Sea Drill. Proj., 81*, 429-438, 1984.

Jones, T. R., and W. K. Parker, On the Rhizopodal fauna of the Mediterranean, compared with that of the Italian and some other Tertiary deposits, *Q. J. Geol. Soc. London, 16*, 292-307, 1860.

Kaminski, M.A., F.M. Gradstein, W.A. Berggren, S. Geroch, and J.P. Beckmann, Flysch-type agglutinated foraminiferal assemblages from Trinidad: Taxonomy, stratigraphy and paleobathymetry, *Abh. Geol. Bundesanst., Austria, 41*, 155-227, 1988a.

Kaminski, M.A., J.F. Grassle, and R.B. Whitlatch, Life history and recolonization among agglutinated foraminifera in the Panama Basin, *Abh. Geol. Bundesanst., Austria, 41*, 229-243, 1988b.

Kaminski, M.A., F.M. Gradstein, D.B. Scott, and K.D. Mackinnon, Neogene benthic foraminifer biostratigraphy and deep water history of sites 645, 646, and 647, Baffin Bay and Labrador Sea, edited by S.P. Srivastava et al., *Proc. Ocean Drill. Program Sci. Results, 105*, 731-756, 1989.

Kastens, K., and J. Mascle, Did a glacioeustatic sea level drop trigger the Messinian Salinity Crisis in the Mediterranean?, edited by P.F. Barker et al., *Proc. Ocean Drill. Program Sci. Results, 113*, 993, 1990.

Keigwin, L.D., Late Cenozoic stable isotope stratigraphy and paleoceanography of DSDP sites of the east equatorial and central North Pacific Ocean, *Earth Planet. Sci. Lett., 45*, 361-382, 1979.

Keigwin, L.D., Neogene planktonic foraminifers from DSDP Sites 502, 503, edited by W.S. Prell et al., *Initial Rep. Deep Sea Drill. Proj., 68*, 269-288, 1982.

Keigwin, L.D., Toward a high-resolution chronology for latest Miocene paleoceanographic events, *Paleoceanography, 2*(6), 639-660, 1987.

Keigwin, L.D., and N.J. Shackleton, Uppermost Miocene carbon isotope stratigraphy of a piston core in the equatorial Pacific, *Nature, 284*, 613-614, 1980.

Keller, G., Late Neogene biostratigraphy and paleoceanography of DSDP Site 310 central North Pacific and correlation with the southwest Pacific, *Mar. Micropaleontol., 3*, 97-119, 1978.

Keller, G., Late Neogene planktonic foraminiferal biostratigraphy and paleoceanography of the northwest Pacific DSDP Site 296, *Palaeogeogr. Palaeoclimatol. Palaeoecol., 27*, 129-154, 1979a.

Keller, G., Late Neogene paleoceanography of the North Pacific DSDP Sites 173, 310, and 296, *Mar. Micropaleontol., 4*, 159-172, 1979b.

Keller, G., Early Pliocene to Pleistocene planktonic foraminiferal datum levels in the North Pacific, DSDP Sites 173, 310, 296, *Mar. Micropaleontol.*, 4, 281-294, 1979c.

Kemp, E.M., L.A. Frakes, and D.E. Hayes, Paleoclimatic significance of diachronous biogenic facies, Leg 28, Deep Sea Drilling Project, edited by D.E. Hayes et al., *Initial Rep. Deep Sea Drill. Proj., 28*, 909-917, 1975.

Kennett, J.P., Recognition and correlation of the Kapitean Stage (upper Miocene, New Zealand), *N. Z. J. Geol. Geophys., 10*, 1051-1063, 1967.

Kennett, J.P., *Marine Geology*, 813 pp., Prentice-Hall Inc., Englewood Cliffs, N.J., 1983.

Knüttel, S., M.D. Russell, and J.V. Firth, Neogene calcareous nannofossils from ODP Leg 105: Implications for Pleistocene paleoceanographic trends, edited by S.P. Srivastava et al., *Proc. Ocean Drill. Program Sci. Results, 105*, 245-262, 1989.

Lincoln, J.M., and S.O. Schlanger, Miocene sea-level falls related to the geologic history of Midway atoll, *Geology, 15*, 454-457, 1987.

Loeblich, A.R. Jr., and H. Tappan, *Foraminiferal Genera and Their Classification*, 970 pp., Van Nostrand Reinhold, New York, 1988.

Loutit, T.S., and L.D. Keigwin, Stable isotopic evidence for latest Miocene sea-level fall in the Mediterranean region, *Nature, 300*, 163-166, 1982.

Loutit, T.S., and J.P. Kennett, Application of carbon isotope stratigraphy to late Miocene shallow marine sediments, New Zealand, *Science, 204*, 1196-1199, 1979.

McDougall, I., N.D. Watkins, and L. Kristjanson, Geochronology and paleomagnetism of a Miocene-Pliocene lava sequence at Bessastadaa, eastern Iceland, *Am. J. Sci., 276*, 1078-1095, 1976.

McKenzie, J.A., and H. Oberhänsli, Paleoceanographic expressions of the Messinian Salinity Crisis, in *South Atlantic Paleoceanography*, edited by K.J. Hsü, and H.J. Weissert, Cambridge Univ. Press, New York, pp. 99-123, 1985.

McKenzie, J.A., H.C. Jenkyns, and G.G. Bennet, Stable isotope study of the cyclic diatomatic claystone from the Tripoli Formation, Sicily: A prelude to the Messinian Salinity Crisis, *Paleogeogr. Paleoclimatol. Paleoecol., 29*, 125-141, 1979.

McKenzie, J.A., D.A. Hodell, P.A. Mueller, and D.W. Mueller, Application of strontium isotopes to late Miocene-early Pliocene stratigraphy, *Geology, 16*, 1022-1025, 1988.

Mercer, J.H., and J.F. Sutter, Late Miocene-early Pliocene glaciation in southern Argentina: Implication for global ice-sheet history, *Palaeogeogr. Palaeoclimatol. Palaeoecol., 38*, 185-206, 1982.

Miller, K.G., R.G. Fairbanks, and G.S. Mountain, Tertiary oxygen isotope synthesis, sea-level history, and continental margin erosion, *Paleoceanography, 2*(1), 1-19, 1987.

Miller, K.G., M.D. Feigenson, J.D. Wright, and B.M. Clement, Miocene isotope reference section, Deep Sea Drilling Project Site 608: An evaluation of isotope and biostratigraphic resolution, *Paleoceanography, 6*(1), 33-52, 1991.

Müller, D.W., and K.J. Hsü, Event stratigraphy and paleoceanography in the Fortuna Basin (South-east Spain): A scenario for the Messinian Salinity Crisis, *Paleoceanography, 2*(6), 679-696, 1987.

Müller, D.W., and P.A. Mueller, Origin and age of the Mediterranean Messinian evaporites: Implications from Sr isotopes, *Earth Planet. Sci. Lett., 107*, 1-12, 1991.

Müller, D.W., D. A. Hodell, and P. F. Ciesielski, Late Miocene to early Pliocene (9.8-4.5 Ma) paleoceanography of the Subantarctic southeast Atlantic: Stable isotopic, sedimentologic, and microfossil evidence, edited by P.F. Ciesielski et al., *Proc. Ocean Drill. Program Sci. Results, 114*, 459-474, 1994.

Murray, J.W., Paleogene and Neogene benthic foraminifers from the Rockall Plateau, edited by D.G. Robert et al., *Initial Rep. Deep Sea Drill. Proj., 81*, 503-529, 1984.

Ocean Drilling Program Leg 151 Shipboard Scientific Party, Exploring Arctic history through scientific drilling, *EOS Trans. AGU, 75*(25), 281, 285, 286, 1994.

Oslick, J.S., K.G. Miller, M.D. Feigenson, and J.D. Wright, Oligocene-Miocene strontium isotopes: Stratigraphic revisions and correlation to the inferred glacioeustatic record, *Paleoceanography, 9*(3), 427-444, 1994.

Perch-Nielsen, K., Cenozoic calcareous nannofossils, in *Plankton Stratigraphy*, edited by H.M. Bolli, J.B. Saunders, and K. Perch-Nielsen, pp. 427-555, Cambridge Univ. Press, New York, 1985.

Phleger, F.B., and F.L. Parker, Ecology of foraminifera, northwest Gulf of Mexico, Part 2, Foraminiferal species, *GSA Mem. Geol. Soc. Am., 46*, 1–64, 1951.

Pirazzoli, P.A., *World Atlas of Holocene Sea-Level Changes, Elsevier Oceanogr. Ser.* vol. 58, 300 pp., Elsevier, New York, 1991.

Pomar, L., and W.C. Ward, Response of a late Miocene Mediterranean reef platform to high-frequency eustasy, *Geology, 22*, 131-134, 1994.

Reuss, A. E., Über die fossilen Foraminiferen und Entomostraceen der Septarienthone der Umgegend von Berlin, *Z. Dtsch. Geol. Gese., 3*, 49-91, 1851.

Roberts, A.P., G.M. Turner, and P.A. Vella, Magnetostratigraphic chronology of late Miocene to early Pliocene biostratigraphic and oceanographic events in New Zealand, *Geol. Soc. Am. Bull., 106*, 665-683, 1994.

Roberts, D.G, Schnitker et al., *Initial Reports of Deep Sea Drilling Project*, vol. 81, 923 pp., U.S. Gov. Print. Off., Washington, D.C., 1984.

Ryan, W.B.F., Geodynamic implications of the Messinian crisis of salinity, In *Messinian Events in the Mediterranean*, edited by C.W. Drooger, pp. 26-38, North-Holland Publishing, New York, 1973.

Ryan, W.B., K.J. Hsü, M.B. Cita, P. Dumitrica, J.M. Lort, W. Maync, W.D. Nesteroff, G. Pautot, H. Stradner, and F.C. Wezel, *Initial Reports of Deep Sea Drilling Project*, vol. 13, parts 1 and 2, 516 pp., U.S. Gov. Print. Off., Washington, D.C., 1973.

Schröder, C.J., Deep-water arenaceous foraminifera in the Northwest Atlantic Ocean, *Can. Tech. Rep. Hydrogr. Ocean Sci. 71*, 191 pp., Minster of Supply and Services Canada, Dartmouth, Nova Scotia, 1986.

Schwager, C., Fossile Foraminiferen von Kar-Nicobar, Reise der Österreichischen Fregatte Novara um Erde in den Jahren 1857, 1858, 1859 unter den Befehlen des Commodore, *Von Wullerstofi-Urbair, Geol. Theil, 2*(1), 187-268, 1866.

Scott, D.B., and G.T. Leger, Benthic foraminifers and implications for intraplate deformation, ODP Site 717, distal Bengal Fan, edited by J.R. Cochran et al., *Proc. Ocean Drill. Program Sci. Results, 116*, 189-206, 1990.

Scott, D.B., and F.S. Medioli, Vertical zonations of marsh foraminifera as accurate indicators of former sea-level, *Nature, 272*, 528-531, 1978.

Scott, D.B., and F.S. Medioli, Quantitative studies of marsh foraminiferal distribution in Nova Scotia, *Spec. Publi. Cushman Found Foraminifer. Res. 17*, 1-58, 1980.

Scott, D.B., and F.S. Medioli, Foraminifera as sea-level indicators, in *Sea-Level Research: A Manual for the Collection and Evaluation of Data*, edited by O. Van de Plassche, GeoBooks, Norwich, pp. 435-455, England, 1986.

Scott, D.B., P.J. Mudie, A. de Vernal, C. Hillaire-Marcel, V. Baki, K.D. MacKinnon, F.S. Medioli, and L. Mayer, Lithostratigraphy, biostratigraphy, and stable-isotope stratigraphy of Cores from ODP Leg 105 Site surveys, Labrador Sea and Baffin Bay, edited by S.P. Srivastava et al., *Proc. Ocean Drill. Program Sci. Results, 105*, 561-581 (+ foldout), 1989.

Scott, D. B., J. R. Suter, and E. C. Kosters, Marsh foraminifera and arcellaceans of the lower Mississippi Delta: Controls on spatial distributions, *Micropaleontology, 37*, 373-392, 1991.

Shackleton, N.J., and J.P. Kennett, Late Cenozoic oxygen and carbon isotope changes at DSDP Site 284: Implications for glacial history of the Northern Hemisphere and Antarctica, edited by J.P. Kennett et al., *Initial Rep. Deep Sea Drill. Proj., 29*, 801-807, 1975.

Shackleton, N.J., M.A. Hall, and D. Pate, Pliocene stable isotope stratigraphy of ODP Site 846, *Proc. Ocean Drill. Program Sci. Results, 138*, 337-355, 1995.

Srinivasan, M.S., and S.N. Chaturvedi, Neogene planktonic foraminiferal biochronology of the DSDP Sites along the Ninetyeast Ridge, northern Indian Ocean, in *Centenary of Japanese Micropaleontology*, edited by K.M. Ishizaki and T Saito, pp. 175-188, Terra Sci., Tokyo, 1992.

Srivastava, S.P. et al., *Proceedings of the Ocean Drilling Program*, vol. 105, part 1, 917 pp. U.S. Gov. Print. Off., Washington, D.C., 1989a.

Srivastava, S.P. et al., *Proceedings of the Ocean Drilling Program*, vol. 105, part 2, 1038 pp., U.S. Gov. Print. Off., Washington, D.C., 1989b.

Stow, D.A., and J.A. Holbrook, Hatton Drift contourites, Northeast Atlantic, Deep Sea Drilling Project Leg 81, edited by D.G. Roberts et al., *Initial Rep. Deep Sea Drill. Proj., 81*, 695-699, 1984.

Talwani, M. et al., *Initial Reports of Deep Sea Drilling Project*, vol. 38, 1256 pp., U.S. Gov. Printi. Off.,Washington, D.C., 1976.

Thomas, F. C., F. S. Medioli, and D. B. Scott, Holocene and latest Wisconsinan benthic foraminiferal assemblages and paleocirculation history, Lower Scotian Slope and Rise, *Micropaleontology, 20*, 212-245, 1990.

Thunell, R.C., Late Miocene-early Pliocene planktonic foraminiferal biostratigraphy and paleoceanography of low latitude marine sequences, *Mar. Micropaleontol., 6*, 71-90, 1981.

Ujiie, H., Bathyal benthic foraminifera in a piston core from east off Miyako islands, Ryukyu Island Arc, *Bull. Coll. Sci.*, Univ. Ryukyus, *49*, 60 pp. + 32 plates, 1990.

Vail, P.R., R.M. Mitchum Jr., and S. Thompson III, Global cycles of relative changes of sea level, in *Seismic Stratigraphy-Application to Hydrocarbon Exploration*, edited by C.E. Payton, *AAPG, Mem., 26*, 83-97, 1977.

Van Couvering, J.A., W.A. Berggren, R.E. Drake, E. Aguirre, and G.H. Curtis, The terminal Miocene events, *Mar. Micropaleontol., 1*, 263-286, 1976.

Van Morkhoven, F.P.C.M., W.A. Berggren, and A.S. Edwards, *Cenozoic Cosmopolitan Deep–Water Benthic Foraminifera*, 421 pp., Elf Aquitaine Press, France, 1986.

Von Fichtel, L., and J. P. C. von Moll, *Testacea microscopica, aliaque minuta ex generibus Argonauta et Nautilus, ad naturam picta et descripta (Microscopische und andere klein Schalthiere aus den geschlechtern Argonaute und Schiffer)*, 123 pp + 24 plates, Camesina (Wien.), 1798.

Wang, P. et al., *Foraminifera and Ostracoda in Bottom Sediments of the East China Sea* (in Chinese with English summary), Ocean Press, Beijing, 438 pp., 1988.

Williamson, W. C., *On Recent Foraminifera of Great Britain*, 107 pp., R. Soc., London, 1858.

Wolf, T.C.W., Paläo-ozeanographisch-Klimatische entwicklung des Nördlichen Nordatlantiks seit dem späten Neogen (ODP Legs 105 und 104, DSDP Leg 81, *Geomar Rep. 5*, 1-92, 1991.

Zhang, J., North Atlantic deep-water circulation during the Messinian Stage - possible cause and effect: Foraminiferal and stable isotopic evidence, Ph.D. thesis, 418 pp., Dalhousie Univ., Halifax, Canada, 1996.

Zhang, J., and D.B. Scott, Integrated stratigraphy and paleoceanography of the Messinian (latest Miocene) across the North Atlantic Ocean, *Mar. Micropaleontol.*, in press, 1996.

D.B. Scott, Centre for Marine Geology, Dalhousie University, Halifax, Nova Scotia B3H 3J5, Canada (e-mail address: dbscott@ac.dal.ca);

J. Zhang, Centre for Marine Geology, Dalhousie University, Halifax, Nova Scotia B3H 3J5 Canada (e-mail address jijun@ac.dal.ca)

(Received June 16, 1995; revised January 31, 1996;
accepted February 21, 1996.)